Aggregate Lapsation Risk*

Ralph S.J. Koijen Hae Kang Lee Stijn Van Nieuwerburgh

December 22, 2022

Abstract

We study aggregate lapsation risk in the life insurance sector. We construct two lapsation risk factors that explain a large fraction of the common variation in lapse rates of the 30 largest life insurance companies. The first is a cyclical factor that is positively correlated with credit spreads and unemployment, while the second factor is a trend factor that correlates with the level of interest rates. Using a novel policy-level database from a large life insurer, we examine the heterogeneity in risk factor exposures based on policy and policyholder characteristics. Young policyholders with higher health risk in low-income areas are more likely to lapse their policies during economic downturns. We explore the implications for hedging and valuation of life insurance contracts. Ignoring aggregate lapsation risk results in mispricing of life insurance policies. The calibrated model points to overpricing on average. In the cross-section, young, low-income, and high-health risk households face higher effective mark-ups than the old, high-income, and healthy.

Keywords: lapsation, insurance, business cycles, hedging
JEL codes: G22, G12, G52, E32, E44

*First Draft: October 2021. Koijen: University of Chicago, Booth School of Business, NBER, CEPR; ralph.koijen@chicagobooth.edu. Lee: Department of Finance, Darla Moore School of Business, University of South Carolina; haekang.lee@moore.sc.edu. Van Nieuwerburgh: Department of Finance, Columbia Business School, Columbia University, NBER, CEPR, ABFER; svnieuwe@gsb.columbia.edu. We gratefully acknowledge data support from the Life Insurance Company. Koijen acknowledges financial support from the Center for Research in Security Prices at the University of Chicago and the Fama Research Fund at the University of Chicago Booth School of Business. For comments and suggestions, we thank Michael Gallary, Daniel Gottlieb, Sears Merritt, and seminar participants at the NBER Summer Institute Household Finance meeting and Rutgers business school.

1 Introduction

Life insurance is a key risk management tool for households when it comes to managing the tail risk associated with the premature death of a family member. Based on a 2016 LIMRA survey, 67% of men and 62% of women between the ages of 35 and 44 own a life insurance policy (see Koijen and Van Nieuwerburgh, 2020). While life insurance holdings increase with income, participation rates are still 66% for men and 70% for women among those earning between $35k and $50k in annual income.

These ownership statistics mask the fact that policyholders frequently lapse (surrender) their policies, thereby forfeiting the insurance protection the policy had afforded. The actuarial literature has found that policyholders often lapse in response to economic hardship. Our focus is on the implications of the link between lapsation and macroeconomic conditions both for the policyholder and the insurer. Despite the presence of this important link and the prevalence of life insurance, life insurance markets and lapsation risk have not received nearly as much attention in the household finance and financial economics literature as, for instance, the mortgage and consumer credit markets.[1]

In this paper, we use new data at the insurer and policyholder level to first develop new measures of aggregate lapsation risk. Next, we show how life insurance contracts with different policy and policyholder characteristics are differentially exposed to these common lapsation factors. We find that young, low-income, and high health-risk households are more likely to lapse their policies recessions, which has long-lasting consequences for their economic well-being and contributes to the cost of business cycles. These new facts also have implications for life insurers, since the systemic variation in lapsation rates affects the valuation and risk mismatch on the balance sheets of insurance companies.[2]

To start, we use regulatory filings data from the 30 largest life insurance companies from 1996 to 2020 to measure the dynamics and co-movement of lapsation rates. We decompose the lapsation rate of each company into a trend and a cycle component. We then extract the first principal component of the trend components and the first principal component of the cycle components. The first principal components explain the bulk of the variation across years and companies. The first factor, which we label the trend factor, captures a secular decline in lapsation rates, from a little over 7% per year in the beginning of our sample to approximately 5% at the end of our sample. The dynamics of this factor follows the trend in the level of interest rates. The second factor captures the counter-cyclicality in lapsation rates. This cycle factor correlates strongly with credit spreads and macroeconomic

[1] An important recent exception is Gottlieb and Smetters (2021).

[2] The impact of lapsation on life insurance valuations is analogous to the impact of prepayment on the valuation of mortgages.

conditions. We illustrate the co-movement between the cycle factor and employment (left panel) and GDP (right panel) in Figure 1.

Figure 1. **Lapse Cycle and Macro Variables**

This figure plots the lapse cycle factor against macroeconomic variables. The red dotted line in both panels represent the lapse cycle factor. The black line in the left panel represents the cyclical component of employment ("Filtered Employment"). The black line in the right panel represents the cyclical component of GDP ("Filtered GDP").

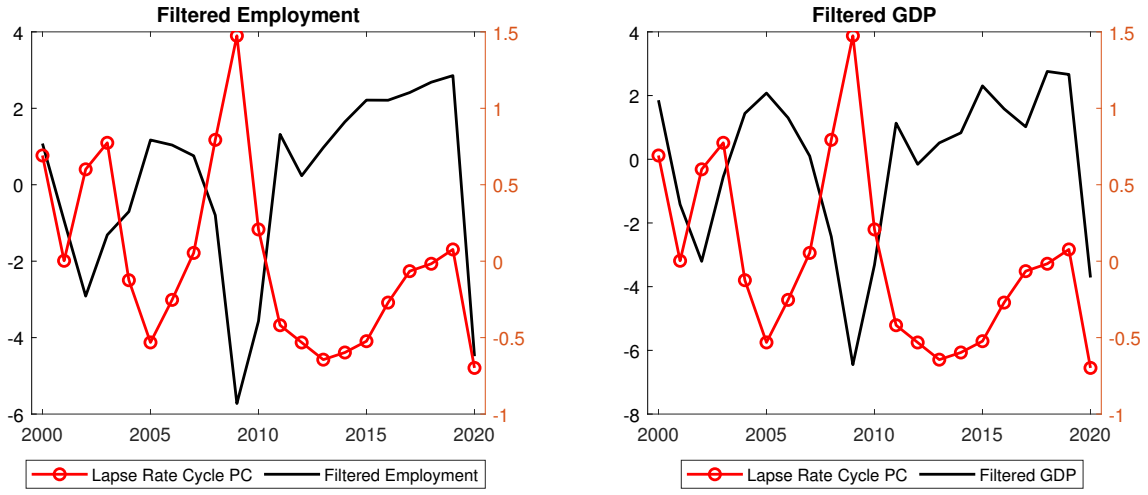

We find additional support for systematic variation in lapsation by exploring geographic variation. In particular, counties with more adverse housing and labor market conditions during the Great Financial Crisis experienced larger increases in the lapse rates.

With the aggregate lapsation factors in hand, we explore how exposure to these factors varies with policy and policyholder characteristics. We exploit a new proprietary data set from a large US life insurance company, the first analysis on such micro data for the United States. We have detailed data on the terms of the life insurance policy (including term or whole life insurance, the length of the term, and the size of the policy) and policyholder characteristics (including age, health status, zip code, and gender).

We estimate a proportional hazard model with policy and policyholder characteristics and their interactions with the lapse cycle. We find that higher health-risk and smoking households have higher lapsation sensitivity to the business cycle. For whole life policies, we find strong dependence on policyholder age and on policy size (death benefit), with younger households and larger policies displaying more sensitivity to the lapse cycle than older households and smaller policies. We cluster households based on demographics, such as income, race, and home-ownership, and find that one cluster containing a high share of minority households of average income is more likely to lapse during economic downturns. The lapsation behavior of a cluster of high-income households is less counter-cyclical. The

behavior across clusters is the same for term and whole life insurance. More broadly, while whole-life policies display stronger cyclicality than term life policies, term life lapsation is clearly counter-cyclical. This is a new finding to the literature, which has focused on whole life lapsation. Since term life policies typically have no cash surrender value, their counter-cyclical lapsation indicates the importance of binding cash-flow constraints for households in recessions. This finding provides a new dimension to the emergency fund hypothesis discussion in the literature, which has focused on the role of the cash surrender value.

These findings are not only relevant to households, but also to life insurance companies. In particular, as a result of the correlation between lapsation and aggregate economic conditions, the valuation of life insurance policies is affected. Since lapsation is high during economic downturns, when investors' marginal utility is high, the effective lapsation rate is higher when accounting for aggregate risk. Formally, the risk-neutral lapsation rate is higher than the physical lapsation rate.

We explore how lapsation rates are reflected in life insurance valuations. There are two opposing forces. On the one hand, when insurance companies underwrite policies, they pay an acquisition fee, typically a commission to the insurance broker. If the policy is more likely to lapse early, the insurer may not yet have recovered the acquisition cost, and ignoring aggregate lapsation risk would lead to a premium that is too low. We refer to this as the "fixed-cost effect." On the other hand, a key feature of typical life insurance contracts is that the premium paid is flat over the life of the contract. Since mortality risk increases with age, insurers profit during the first years of the contract (when the cost of mortality cover is below the premium) and lose money during the later years of the contract (when the cost of mortality cover exceeds the premium). If insurers ignore aggregate lapsation risk, and use a lapsation rate that is too low, they put too much weight on the later years of the contract that are unprofitable. The insurance premium charged would therefore be too high. We refer to his as the "mortality effect."

Given these opposing forces, it is a quantitative question how aggregate lapsation risk affects life insurance valuation. We develop an asset pricing model that captures the observed correlation of lapsation rates with financial market variables. The model is calibrated to match the prices of Treasury and corporate bonds. We find that the mortality effect outweighs the fixed-cost effect. In our calibration, premiums on a 20-year life insurance contract sold to a healthy 40-year old are about 3% higher than they would be if the contract was correctly priced, while insurer profits are about 30% too high. Excess profits are higher in a low interest rate environment.

To the extent that the heterogeneity across policyholders in exposures to the lapsation cycle is not reflected in the pricing of life insurance, which our conversations with industry experts confirm, ignoring aggregate lapsation risk also has important implications for the

cross-section of policies. Specifically, the young, higher health-risk policyholders, living in lower-income and higher-minority share areas, who have the highest exposure to the lapse cycle, face the most overpriced policies. Older, richer, and healthier policyholders face the least overpriced policies. For a given markup on the insurer's book of business, the former group effectively subsidizes the latter group. Since the former group has higher marginal utility than the latter, ignoring lapsation risk (inadvertently) results in "wrong-way-around" redistribution. Furthermore, the cross-sectional pricing effects could affect both the extensive and the intensive margin of coverage.

The COVID-19 pandemic, which occurs at the end of our sample, presents an interesting study in contrasts. Unlike in previous recessions, the lapsation rate falls in 2020. We conjecture that, first, the coronavirus increased the salience of mortality risk, and brought renewed urgency to not letting insurance policies lapse, and second, that the government's unusually generous transfer spending (stimulus checks, extended unemployment insurance) enabled households to continue paying their insurance premiums in the face of economic hardship. Government emergency funds alleviated the need to use the life insurance policy as an emergency fund, and preserved the financial protection life insurance provides to households.

Our findings have implications for the design of life insurance policies. As the increase in lapsation is plausibly related to binding financial constraints at the household level, an interesting question is how to optimally design life insurance policies that account for aggregate risk. While policies with cash values and the ability to lend against them can buffer some of the shocks, we find that lapsation also increases for term life policies during economic downturns. Premium holidays in recessions would reduce lapsation and benefit households, but would affect pricing (especially in a model with aggregate risk) and could potentially hurt the financial stability of the insurance sector.[3] In short, our paper raises interesting questions for contract design, and how those might interact with behavioral frictions documented recently in Gottlieb and Smetters (2021).

Related Literature Along with mortality, lapsation behavior is a key risk factor in the pricing of life insurance policies and has been studied extensively in the insurance literature. Most of the discussion focuses on whole life policies, which pay the policyholder an amount, known as the cash surrender value, upon lapsation. The emergency fund hypothesis (EFH), going back to Linton (1932), hypothesizes that personal financial distress (a negative income or unemployment shock) may result in lapsation since the policyholder may want to access the cash surrender value for consumption smoothing purposes. The second and third main hypotheses are the interest rate hypothesis (IRH, Schott (1971)) and policy replacement hy-

[3]See Greenwald, Landvoigt, and Van Nieuwerburgh (2021) for a related discussion in the context of shared-appreciation mortgages whose payments are tied to (aggregate or regional) house prices.

pothesis (PRH, Outreville (1990)), which are related. They state that when interest rates go up, policies are more likely to lapse because policyholders may want to walk away from their current policy–whose investment account was earning a lower fixed rate– and turn to a higher-yielding investment or a new life insurance policy (with higher implicit return or lower premium payments) instead.[4] See Eling and Kochanski (2013) and Bauer et al. (2017) for recent reviews.

These hypotheses have been tested empirically, initially in aggregate time-series data. Evidence for the U.K. (Dar and Dodds, 1989), the U.S. and Canada (Outreville, 1990; Kuo, Tsai, and Chen, 2003), South Korea (Kim, 2005), and Germany (Kiesenbauer, 2012; Kubitza, Grochola, and Grundl, 2022) is generally supportive of both the EFH and the IRH. Lapsation tends to increase with both aggregate unemployment and with interest rates, with the relative strength depending on the country, sample, and empirical method. We extend this analysis by studying a more recent data sample, which includes the Great Financial Crisis and the COVID-19 crisis, and we apply a novel method that extracts an aggregate lapsation cycle and trend from firm-level data. Our results provide strong support for both the EFH and IRH.

A more recent, and much smaller strand of the empirical literature uses individual-level policy data to analyze lapsation behavior. Fier and Liebenberg (2013) uses the Health and Retirement Survey in the U.S. to study voluntary lapsation. It finds that negative income growth (but not unemployment) is associated with higher lapsation, consistent with the EFH, and that individuals who obtained a new life insurance policy are more likely to have lapsed, consistent with the PRH. Households that lost their bequest motive due to death of a spouse, divorce, or retirement are more likely to lapse. Lapsation first increases and later declines in age, while income is not significant. Sirak (2015) uses data from a German life insurance company and estimates a proportional hazard model to find strong evidence for the EFH. Income drives out policyholder age and education. The PRH may be less relevant in an era of declining interest rates and in a context with high surrender fees.

Using U.S. HRS data, Fang and Kung (2021) find that many lapsation decisions are driven by idiosyncratic shocks, uncorrelated with health, income, and bequest motives, especially for younger policyholders. Likewise, Gottlieb and Smetters (2021) find evidence based on a survey instrument for forgetfulness as an important driver of lapsation, alongside with negative income shocks (or liquidity needs more generally) which policyholders tend to underestimate. Society of Actuaries and LIMRA (2019) and Milliman (2020) provide industry studies of lapsation behavior of member firms and analyze its determinants.

In this paper, we study individual-level lapsation data for the U.S. from a large U.S.

[4] Hendel and Lizzeri (2003) show how the front-loading of insurance policies affects lapse behavior by comparing renewable term policies to level-payment term policies.

life insurance company. Importantly, we focus on *heterogeneity* across policyholders in their *exposure to the lapse cycle*. Not only do policy and policyholder characteristics matter for lapsation, we find systematic variation in the sensitivity of lapsation to the cycle depending on policyholder age, risk status, and income. Private conversations with industry experts reveal that models with individual lapsation determinants do not consider cyclicality in lapsation. Hence, the interaction of individual characteristics with lapsation in the data but not in the models used for pricing implies important redistributional effects across policyholders. While it is stronger for whole than for term life, our finding that term life lapsation rates are also counter-cyclical is new and sheds a new light on a lapsation literature that has been focused on whole life policies.

Finally, we contribute by developing a tractable affine model of life insurance valuation that models lapsation as a function of the interest rate and the cycle (credit spread). We contribute to the theoretical literature by explaining how cyclical lapsation affects the pricing of term life policies, and what the role of the interest rate is.

The lapsation literature has interesting parallels to the much larger literature on mortgage prepayment and valuation in finance (E.g., Schwartz and Torous, 1989; Stanton, 1995; Deng, Quigley, and Order, 2000; Boyarchenko, Fuster, and Lucca, 2019; Chernov, Dunn, and Longstaff, 2018; Diep, Eisfeldt, and Richardson, 2021). In this literature, it is well understood that modeling prepayment risk and the covariance of prepayment rates with priced aggregate risk factors is essential to determine the correct valuation of a mortgage or a pool of mortgages (mortgage-backed security). Real-world mortgage prepayment behavior responds to interest rates (the rate incentive) and variables that move with the business cycle like employment or house prices, which affect turnover in the housing and hence mortgage market. But prepayment also contains behavioral aspects that are harder to capture with a rational model. In another parallel, the recent mortgage literature has emphasized that suboptimal prepayment behavior can lead to cross-subsidization and redistribution (Gerardi, Willen, and Zhang, 2021; Zhang, 2022; Fisher et al., 2021). We show that lapsation rates are also exposed to priced aggregate risks, that accounting for these aggregate risks is important in computing insurance premiums, and that cross-sectional differences in actual lapsation behavior have distributional consequences when they are not reflected in insurance premiums.

2 Data and Empirical Methodology

2.1 Data

2.1.1 S&P Global Market Intelligence

To study aggregate lapsation risk, we analyze two databases. The first database is S&P Global Market Intelligence (SNL), which contains the universe of regulatory filings by insurance companies. We focus on life insurance companies and exclude property and casualty insurance companies. The data are at the annual frequency, spanning 1996 to 2020 (the lapse rate starts in 1997). SNL offers data at two different levels of granularity: at the company level (company codes starting with "C") or at the group level (company codes starting with "GK"). We use group-level data in our baseline analysis. For robustness, we also repeat the same analysis using corporate-level data, and find that the analysis does not meaningfully change. We refer to *firm* or *firm-year* to represent the entities in the group-level data (that is, "GK" companies).

The main variable of interest is the lapsation rate observed at a yearly frequency. We use the term "lapsation rate" to include both the lapsation and surrender, following the standard definition used in the industry (Society of Actuaries and LIMRA, 2019). We use the lapsation rate for ordinary life insurance (that is, individual life insurance), retrieved from the *Ordinary Life: Lapse & Surrender Ratio* time series of the SNL dataset.[5] We drop the following five insurance groups: SCOR U.S. Only (GK4020905), RGA U.S. Only (GK103450), Swiss Re U.S. Only (GK4290308), Hannover Life Reassurance (C2749), and Munich Re U.S. Only (GK4005715). These companies are either international or reinsurance companies. For the regression analysis, we drop outliers with lapsation rates greater than 30%, which removes 2.8% of the lapsation rate observations. The 30 largest firms in the SNL database represent about 81.2% of the market based on the in-force policy size at the end of 2020.

2.1.2 Macro Variables

We construct two macro variables, GDP and Employment, at the firm-year level. Specifically, we start from state-level macro time series data from the FRED database of the St. Louis Fed. For GDP, we use the annual *Real Total Gross Domestic Product* series for each state. The time series starts in 1997. We extend this series back to 1993 by regressing GDP growth rates of each state on state-level employment growth rates and the aggregate GDP growth rate.

[5] Data is accessed on April 18, 2021. Note that S&P Global Market Intelligence retrospectively updates historical financial data to reflect the latest corporate structures following M&As and other corporate activities. In "Group Methodology Summary on MI" document, it states *"Market Intelligence Groups are composed of members within that corporate structure on an as-is basis. Structures are updated quarterly and amended for any mergers or acquisitions. The current members' composition is applied retrospectively to all financial data for all periods."*

We then apply the Hamilton (2018) filter to the annual series of the state-level log GDP to obtain its cyclical component.[6] For Employment, we use the seasonally-adjusted monthly *All Employees: Total Nonfarm* time series for each state. We apply the Hamilton filter to the log level of employment, and take the annual average of the filtered values. For each firm-year, we use the share of total life insurance premium income (*Life ex Annuity: Sate Direct Premiums & Annuity Considerations (in $000)* from S&P Global Market Intelligence) in each U.S. state as the weight vector to calculate firm-specific macro variables. This process generates our firm-year level macro time series.

Aggregate macro variables are also retrieved from the FRED database of the St. Louis Fed. For GDP, we use the annual *Real Gross Domestic Product* series (GDPCA). We apply the Hamilton filter to the annual series of the log GDP. For employment, we first retrieve the monthly *All Employees, Total Nonfarm* series (PAYEMS), and apply the Hamilton filter to the monthly series to decompose the trend and the cycle. We then take the annual average of the monthly cycle to construct an annual employment cycle series.

For interest rates, we use the *10-Year Treasury Constant Maturity Rate* (GS10), where we convert the monthly series into an annual one by taking averages. For credit spreads, we use *Moody's Seasoned Baa Corporate Bond Yield Relative to Yield on 10-Year Treasury Constant Maturity* (BAA10YM) and follow similar procedure to obtain an annual time series. We average these series because the annual lapsation rate reflects lapsation that occurs throughout the year.

For the county-level analysis, we use the median house price from Zillow. Specifically, we take the average of the monthly ZHVI index over each year to construct the annual series. The county-level unemployment rate data is downloaded from the BLS Local Area Unemployment Statistics (LAUS) and is already at annual frequency.

2.1.3 Policy-level Insurance Database

The second and main novel proprietary database is provided to us by a major U.S. life insurance company. This is a large database of life insurance contracts, containing policy-level details. The database is de-identified by a third party vendor for research purposes, so that we cannot recover the identity of policyholders. We observe policy characteristics, such as size, policy type (whole life, term life, or other), policy status (in-force, lapsed, or surrendered) and issuance date. We also observe detailed policyholder characteristics such as age,

[6] The Hamilton filter described in Hamilton (2018) can be applied to both annual and monthly time series with different choices of (h, p) for the regression $y_{t+h} = d_0 + \sum_{j=1}^{p} d_j y_{t-j+1} + c_{t+h}$. We use the recommended parameter value of $h = 2$ for annual series and $h = 24$ for monthly series. We also use $p = 2$ for annual series and $p = 12$ for monthly series, which look back one year for the lagged regressors, consistently with the recommended choice of $p = 4$ for quarterly series.

gender, smoking status, risk class, and ZIP code. Hereafter, we will refer to this database as the *Firm Database* for convenience. The database contains life insurance policies originated between late 1998 and early 2016.

As part of our data validation process, we compare the lapse rates of the Firm in the S&P database (see Section 2.1.1) with the aggregate lapse rates we construct using the Firm Database. If the Firm Database is representative of the firm's portfolio of insurance policies, the two lapsation rates should be close. We present a comparison in Figure 2. The orange line plots the lapsation rate from the S&P database, while the blue line plots the aggregate lapse rate calculated from the Firm Database. In the early period from 1999–2004, there is a wide discrepancy between the two lines. This discrepancy is due to the left-truncation of the Firm Database, which only contains new policies originated after late-1998. To see this, note that the lapse rate in year t is calculated using the following equation:

$$LapseRate_t = \frac{\text{Policies Lapsed within Year } t}{0.5\,(\text{In-Force Beginning of Year } t + \text{In-Force End of Year } t)} \tag{1}$$

where the numerator and the denominator can be based on either the number of policies or the amount of face value.

Since we only observe the policies issued by the *Firm* on or after 1998, it takes a few years until the in-force policy pool populates and the denominator stabilizes. Similarly, at the end of the sample, the two lines diverge as we do not observe policies in the firm-level database that were originated after 2016. In between these two periods, our firm-level data set tracks the aggregate lapse rate well.

We merge in ZIP-code level income data from the 2016 IRS SOI Tax Stats Data by cacu-lating the average Adjusted Gross Income. Additionally, the ZIP-code level race, education, and homeownership data is retrieved from the Census.[7] We merge in the ZIP-code level Census data to construct *Minority* variable to measure the fraction of Black or Hispanic population,[8] *College+* variable to measure the fraction of population with bachelor's degree or higher, and *HomeOwnership* variable to measure the fraction of homeowners within the ZIP codes.

[7]Census data is retrieved from 2016 5-year American Community Survey, accessed in August 2022. Race, education, homeownership information are retrieved from B03002, S1501, and DP04 tables, respectively.

[8]Note that being Hispanic is an ethnic concept, we remove the double-counting of Black-Hispanic population.

Figure 2. **Aggregate Lapse Rate Validation**

This figure presents the validation exercise we perform to ensure the coverage of the Firm Database we use. The blue line plots the aggregate lapse rate we directly calculate from the Firm Database using Equation (1). The orange line plots the reported aggregate lapse rate from the S&P Global Market Intelligence database. Two graphs are reasonably close after 2003, which validates our use of the database. There is some discrepancy early in the period due to left truncation of the database, see Section 2.1.1 for details.

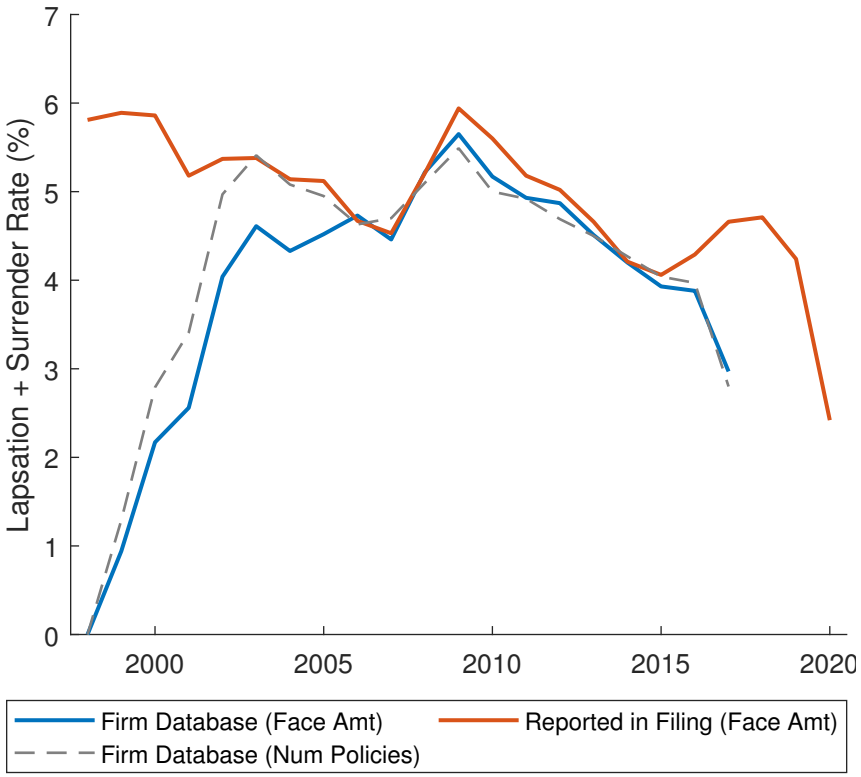

2.2 Empirical Methodology

2.2.1 Principal Component Analysis

For each of the 30 largest[9] life insurance companies, as defined by in-force policy amount outstanding as of 2020, we decompose the lapse rate time series into a trend and cycle component using the Hamilton filter. We then separately run two principal component analyses, one using the trend time series and one using the cycle time series. Starting from the 30 trend time series, we construct the first principal component that explains most of the variation using the correlation matrix, and denote it as the *Lapse Trend factor*. Similarly, we define the

[9]We skip the 30th largest life insurance company, Resolution Life Holdings Inc (GK26554449), because it has the 2010 lapsation rate missing. Instead we include the next largest company, Penn Mutual (GK110258). The PCA results do not fundamentally change when we use the Resolution Life Holdings Inc with the overridden lapsation rate 0.80% for 2010, which is the best estimate based on the *Insurance In Force*, *Insurance Lost: Lapsed* and *Insurance Lost: Surrendered* variables.

Lapse Cycle factor as the first principal component of the 30 cycle time series. We use the *Lapse Trend factor* and the *Lapse Cycle factor* as the aggregate lapsation risk factors.

2.2.2 Firm-level Lapsation Analysis

We first study the heterogeneity in aggregate lapsation risk exposure at the firm-level. The firm-level time series of lapsation rates can be used to run the following factor regression with the lapsation risk factors constructed in 2.2.1:

$$Lapse\,Rate_t^j = \alpha^j + \beta^j_{Trend} Lapse\,Trend_t + \beta^j_{Cycle} Lapse\,Cycle_t + \varepsilon^j_t, \tag{2}$$

where j represents the index for firm j.

2.2.3 Geographical Analysis

We investigate the geographical variation in lapse rate changes between 2006 and 2009 at the county-level. As the severity of the economic downturn varies across geographies, it provides us another way to explore how economic conditions relate to lapse rates. Specifically, we study the relationship with county-level economic variables such as house price changes and unemployment rate changes. The *Firm Database* contains the policyholders' ZIP codes for about 95% of our sample, so we first map the ZIP code information to the corresponding county's FIPS code by using the HUD USPS ZIP code-to-county crosswalk.[10] There are 3,049 counties in the database, and the *Firm*'s life insurance business is concentrated in larger and more populous counties. As the lapsation calculation becomes noisy for counties with little coverage, we drop counties with fewer than 100 policies issued in our sample. This leaves us with 826 counties, representing 96% of life insurance face amount coverage of the overall sample. Data on changes in house prices from Zillow (ZHVI) are available for 762 counties (92%), changes in unemployment rates are available for 823 counties (99.6%), and both variables are available for 759 counties (92%). Our results are not sensitive to reasonable variations in the 100-policy threshold.

We construct three county-level variables to measure the change in lapsation rates, hous-

[10] https://www.huduser.gov/portal/datasets/usps_crosswalk.html. We use the union of 2010, 2013, 2016 and 2019 Q1 versions, where the latest mappings were used per ZIP code.

ing prices, and the unemployment rates between 2006 and 2009,

$$
\begin{aligned}
(\Delta Lapse\,06-09)_c &= (Lapse_{c,2009} - Lapse_{c,2006}) \times 100, \\
(\Delta HousingPrice\,06-09)_c &= \left(\frac{ZHVI_{c,2009}}{ZHVI_{c,2006}} - 1\right) \times 100, \\
(\Delta Unemp\,06-09)_c &= (Unemp_{c,2009} - Unemp_{c,2006}) \times 100.
\end{aligned}
$$

We then regress $(\Delta Lapse\,06-09)_c$ on the house price change and the change in the unemployment rate. The baseline specification is least squares, where observations are weighted by the average in-force amount in 2006. This variable is the denominator used in the lapse rate calculation formula. Intuitively, it represents the size of insurance business in each county as of 2006.

2.2.4 Policy-level Lapsation Analysis

For our main analysis, we investigate the heterogeneity in exposures to aggregate lapse risk factors by policy and policyholder characteristics, utilizing the micro-level *Firm Database*. To this end, we estimate a Cox proportional hazard model of the observed lapse events on the time-varying characteristics. For policy j issued at time t, we specify the annual lapsation hazard rate at time $t+n$ as:

$$
\lambda_{j,t}^{(n)} = \lambda_0(n) \exp(\boldsymbol{\beta' Z_{j,t+n}}), \tag{3}
$$

where $\lambda_0(n)$ is the baseline hazard rate at policy age $n \geq 1$, and the log relative risk is linear in the vector of characteristics $Z_{j,t+n}$. We use the policy size (in 2016 USD) as the weight, where we winsorize the smallest 1 percent and the largest 1 percent in our sample. Most of the policy or policyholder characteristics (for instance, gender, smoking status, risk class, and term life policy indicator) are time-invariant. For each policy or policyholder characteristic z_j^i (or $z_{j,t+n}^i$ for time-varying characteristics), we additionally include the interaction term with the lapse cycle factor, i.e. $z_{j,t+n}^{i,cycle} = z_j^i \times (Lapse\,Cycle)_{t+n}$ in the characteristic vector $\boldsymbol{Z_{j,t+n}}$. The estimated coefficients on these interacted variables allow us to understand how the exposure to the cycle factor varies with policy and policyholder characteristics.[11]

[11] We do not include the uninteracted lapse trend factor in the specification because of the left-truncation of the *Firm Database* as described in Section 2.1.3, which results in the divergence of early-2000s in Figure 2.

3 Empirical Results

3.1 Lapsation Trend and Cycle

Following the empirical procedure described in Section 2.2.1, we construct two lapsation risk factors from the 30 lapse trend components and the 30 lapse cyclical components. Figure 3 plots the aggregate lapsation risk factors. The *Lapse Trend factor*, which is the first principal component of the lapse trend time series, explains 96.4% of variation in firms' lapse trends. The *Lapse Cycle factor* explains 69.5% of variation in firms' lapse cycles. These two factors explain a large part of the common variation in lapsation rates across firms, and we use these factors as the aggregate lapse risk factors.

Figure 3. **The Evolution of Lapse Trend and Lapse Cycle**

This figure plots the aggregate lapsation factors we construct. For each company, we start from the historical lapse rate series from 1997 to 2020, and apply Hamilton filter to decompose the lapse rate time series into the trend time series and the cycle time series. We then separately run two principal component analyses to the trend time series and the cycle time series. Starting from the 30 trend time series, we construct the first principal component that explains the most of the variations using the correlation matrix, and denote it as the *Lapse Trend factor*. Similarly, we define the *Lapse Cycle factor* as the first principal component of the 30 cycle time series.

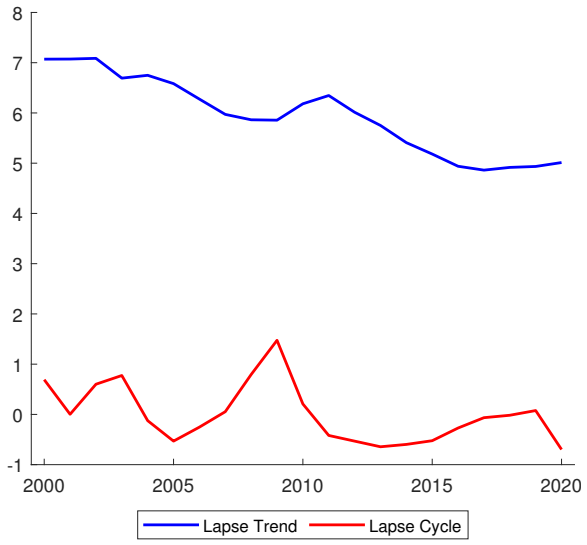

One salient fact is the gradual decline in the *Lapse Trend factor*. Coinciding with the secular decline in interest rates, lapse rates have also been declining over the past 20 years as depicted for several large firms in Figure 4. The *Lapse Trend factor* captures this industry-wide decline. The co-movement with interest rates is illustrated in the upper panel of Figure 5.

Table 1 formalizes this relationship by regressing the *Lapse Trend factor* on the 10-year

Treasury rate and other business cycle variables such as aggregate Filtered GDP, aggregate Filtered Employment, and the Baa credit spread over the 10-year Treasury rate. The positive and statistically significant coefficients on the 10-year Treasury rate, along with insignificant coefficients on the business cycle variables indicate that the *Lapse Trend factor* primarily moves with interest rates.

Lower rates increase the present value of the death benefit, and hence the value of a life insurance contract, making it more costly to lapse from the policyholder's perspective. Lower rates also increase the cost (premium payments) of a new policy, again increasing the cost of lapsing an existing contract that was signed when rates were higher. Finally, and as emphasized in the literature, fixed-rate investment returns on whole life policies signed when rates were higher are attractive relative to the investment returns on new policies (interest rate hypothesis), making it less desirable to replace the old policy with a new one (policy replacement hypothesis). Our evidence is consistent with the IRH and PRH. We do caution that identifying relationships between trending variables is challenging, and we therefore interpret this evidence as suggestive of a link between the trends in lapsation rates and interest rates. That said, the interpretation is bolstered by the evidence from historical records, which showed gradual increases in lapsation rates from the early 1950s until the mid 1980s when interest rates rose, and persistent declines after the mid 1980s when rates started to fall (Kuo, Tsai, and Chen, 2003).

The *Lapse Cycle factor* on the other hand mostly captures the business cycle effect. Figure 1 plots the *Lapse Cycle factor* against two filtered macro variables, employment and GDP. The counter-cyclicality of the *Lapse Cycle factor* is clear from the graphs.[12] The lower panel of Figure 5 shows that the factor is positively correlated with the Baa credit spread, a financial market variable known to be closely related to the business cycle.

Table 2 formalizes this relationship by estimating similar models as in Table 1. Two observations are notable compared to the results in Table 1. First, the coefficients on the business cycle variables, Filtered GDP, and the Baa Credit Spread over the 10-year Treasury yield are all statistically significant at the 5% level, and the coefficient on Filtered Employment is statistically significant at the 10% level. The signs of the coefficients highlight the strong counter-cyclicality of the *Lapse Cycle factor*. Second, the coefficients on the 10-year Treasury yield are also statistically significant and positive. This indicates that the cyclical component of lapsation contains some exposure to declining interest rates.[13] Intuitively, the rise in the lapsation rate in recessions indicates that a subset of policyholders face economic hardship

[12]The principal component analysis is agnostic on the sign of the factor. We construct the factor to be countercyclical instead of being procyclical.

[13]The *Lapse Trend factor* and the *Lapse Cycle factor* are *not* constructed as the first and the second principal component of a set of vectors, so there is no guarantee that these factors are uncorrelated. The constructed lapsation risk factors are positively correlated.

Table 1. **Time Series Regression of Lapse Trend**

This table presents the results of the following time-series regressions:

$$Lapse\ Trend\ Factor_t = \beta\,(\text{Treasury 10y})_t + \gamma X_t + \varepsilon_t$$

for year t, where the business cycle variable X_t indicates either the Filtered GDP, Filtered Employment, or Baa Credit spread over 10y. Robust standard errors are reported in parentheses.

	(1)	(2)	(3)	(4)	(5)
Treasury 10y	0.478***	0.479***	0.465***	0.506***	0.470***
	(0.0688)	(0.0607)	(0.0578)	(0.0608)	(0.0544)
Filtered GDP		-0.0622			0.298***
		(0.0366)			(0.0769)
Filtered Employment			-0.0849**		-0.301***
			(0.0377)		(0.0520)
Baa Credit Spread over 10y				0.306	0.445**
				(0.185)	(0.180)
Constant	4.359***	4.351***	4.401***	3.463***	3.244***
	(0.266)	(0.239)	(0.233)	(0.565)	(0.455)
Observations	21	21	21	21	21
R^2	0.664	0.704	0.735	0.724	0.814
Adjusted R^2	0.646	0.671	0.706	0.693	0.768

Standard errors in parentheses

* p<0.1, ** p<0.05, *** p<0.01

that no longer allows them to make premium payments. Hence, this evidence is consistent with the emergency fund hypothesis (EFH).

The top panel of Figure 5 plots the *Lapse Trend factor* against the 10-year Treasury yield. The bottom panel of Figure 5 plots the *Lapse Cycle factor* against the Baa credit spread over the 10-year Treasury yield.

Table 2. **Time Series Regression of Lapse Cycle**

This table presents the results of the following time-series regressions:

$$Lapse\,Cycle\,Factor_t = \beta\,(\text{Treasury 10y})_t + \gamma X_t + \varepsilon_t$$

for year t, where the business cycle variable X_t indicates either the Filtered GDP, Filtered Employment, or Baa Credit spread over 10y. Robust standard errors are reported in parentheses.

	(1)	(2)	(3)	(4)	(5)
Treasury 10y	0.210***	0.213**	0.195**	0.262***	0.255***
	(0.0549)	(0.0772)	(0.0807)	(0.0620)	(0.0694)
Filtered GDP		-0.124**			-0.113
		(0.0515)			(0.0976)
Filtered Employment			-0.106*		0.0597
			(0.0608)		(0.0859)
Baa Credit Spread over 10y				0.550***	0.366**
				(0.177)	(0.162)
Constant	-0.697***	-0.714**	-0.645**	-2.309***	-1.813***
	(0.186)	(0.279)	(0.300)	(0.581)	(0.548)
Observations	21	21	21	21	21
R^2	0.227	0.504	0.422	0.568	0.596
Adjusted R^2	0.186	0.449	0.358	0.520	0.495

Standard errors in parentheses

* p<0.1, ** p<0.05, *** p<0.01

Figure 4. **Lapse Rates vs. Macro Variable (GDP) of the Largest Life Insurers**

This figure plots the historical lapse rates against the firm-specific filtered GDP of the 12 largest insurance groups from the S&P Global Market Intelligence Database. For each life insurance company, the company-relevant GDP is calculated as the weighted-average of the state-level GDP, where the weights are based on the gross premium income from each state to reflect the economic exposures to each state.

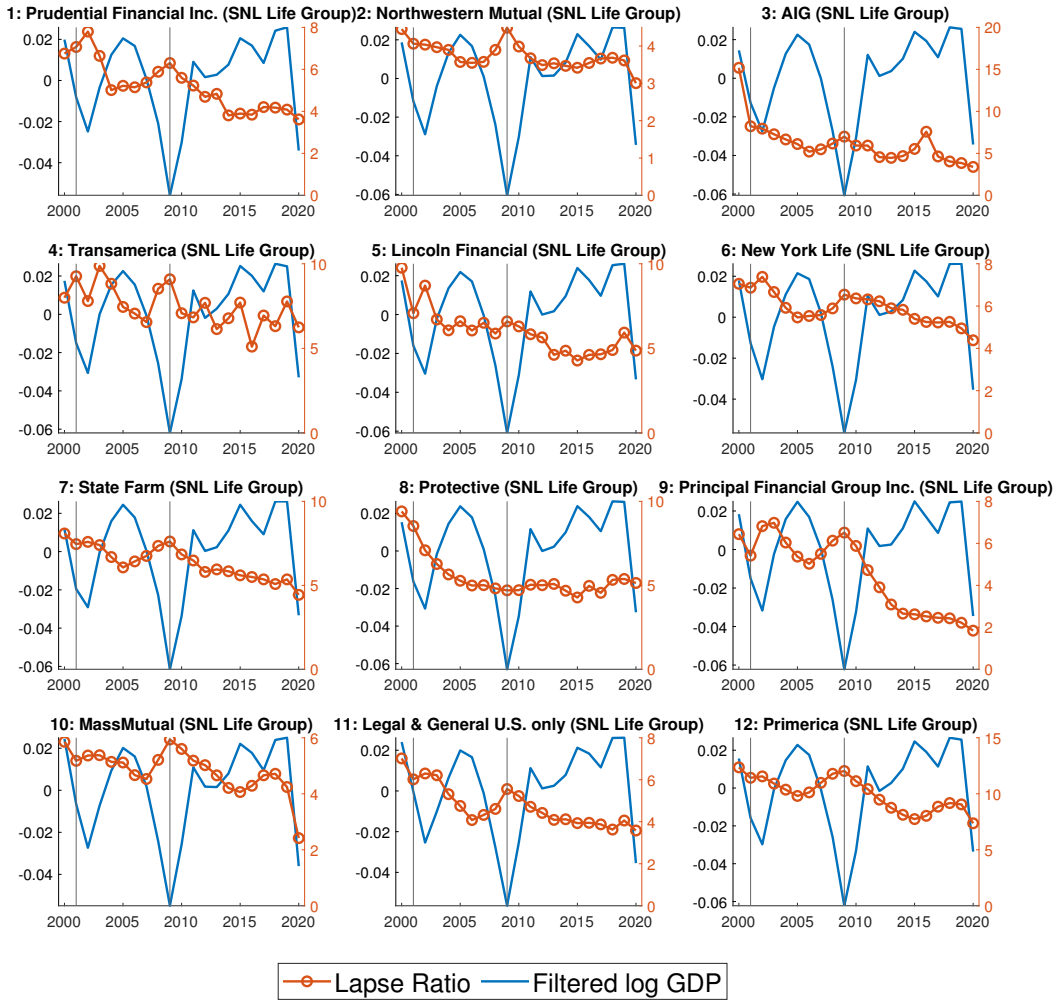

Figure 5. **Lapse Factors and Financial Market Variables**

This figure plots the lapsation factors against the financial market variables. The blue line in the upper panel plots the *Lapse Trend factor* against the 10-year Treasury yield. The red line in the lower panel plots the *Lapse Cycle factor* against the Baa credit spread over 10-year Treasury yield.

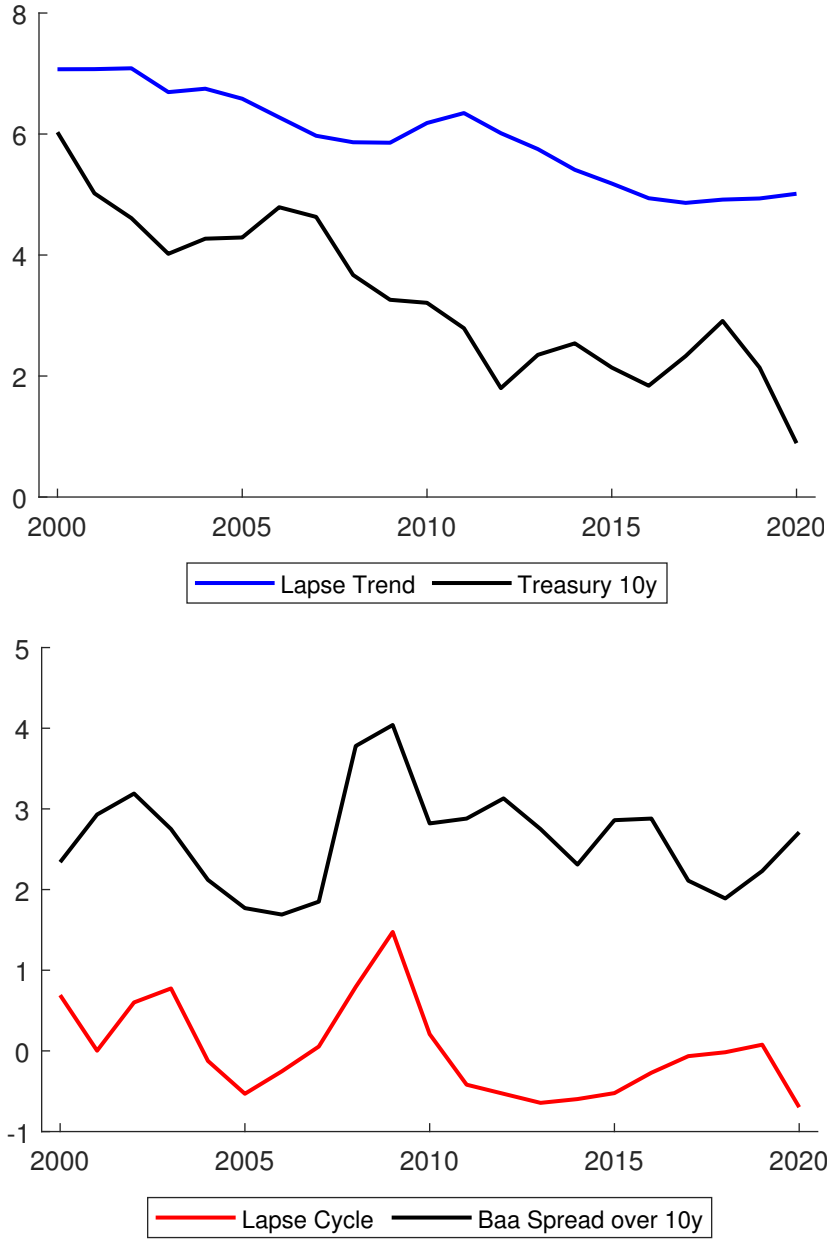

3.1.1 Implications For Hedging

The strong comovement suggests that aggregate lapsation risk can be hedged with a portfolio of Treasuries and corporate bonds. We formalize this intuition in Table 3 by regressing the change in lapse rates on the changes in financial market variables. Unlike in Table 1 and 2, we use changes in variables to establish the relationship, because the changes in variables are more relevant than the levels for hedging purposes. Column (1) suggests that the *Lapse Trend factor* is harder to hedge annually, and that there is a lower frequency relationship between the *Lapse Trend factor* and the 10-year Treasury Rate. Column (2) shows that the annual changes in *Lapse Cycle factor* can be effectively hedged using Baa-rated corporate bonds and Treasuries. In Column (3), we use the change in *Lapse Total* as a dependent variable, which is the sum of the *Lapse Trend factor* and the the *Lapse Cycle factor*. This final column shows that this simple hedging strategy already captures nearly 40% of the variation in lapse rates.

Table 3. **Hedging Opportunities using Financial Products**

This table presents the time-series regression results of the changes in lapsation risk factors on the change in 10-year Treasury rate and the change in Baa Credit Spread over 10-year Treasury yield. Robust standard errors are reported in parentheses.

	(1) ΔLapse Trend	(2) ΔLapse Cycle	(3) ΔLapse Total
ΔTreasury 10y	-0.103	0.551**	0.449**
	(0.124)	(0.224)	(0.158)
ΔBaa Credit Spread over 10y	-0.0897	0.693***	0.603***
	(0.117)	(0.188)	(0.0963)
Constant	-0.128***	0.0594	-0.0682
	(0.0432)	(0.0885)	(0.0875)
Observations	20	20	20
R^2	0.061	0.392	0.394
Adjusted R^2	-0.049	0.320	0.323

Standard errors in parentheses
* p<0.1, ** p<0.05, *** p<0.01

3.2 Heterogeneity in Risk Factor Exposures Across Firms

Equipped with the two aggregate lapsation risk factors, we investigate the heterogeneity in lapsation risk exposures across large life insurers by estimating the regression specified in Equation (2).

Table 4 presents the first set of results for large insurers. The table lists the 30 largest life insurers based on the in-force policy amounts at the end of 2020, which is the same group of life insurers that we used to construct the lapsation risk factors in Section 2.2.1. The third and the fourth column report the mean and the standard deviation of the historical lapse rates. The fifth column reports the correlation of the historical lapse rate series with the filtered employment series. The correlation coefficients are mostly negative, which is consistent with Figure 4. The sixth and the seventh column are the main results of interest: the exposures to the *Lapse Trend factor* and the *Lapse Cycle factor*. We note substantial variation in these risk exposures across companies. This suggests that optimal hedging strategies to manage lapsation risk vary across companies. The valuation impact of aggregate lapse risk similarly varies across companies.

3.3 Geographical Heterogeneity During the Great Financial Crisis

Next, we explore the heterogeneity in lapsation rates across geographies during the 2008 financial crisis. Figure 6 presents the binscatter plots of the county-level lapse rate change, $(\Delta Lapse\, 06-09)_c$, against the county-level economic variables during the Great Financial Crisis. The top panel plots the lapse rate change against the housing price change, $(\Delta Housing\ Price\, 06-09)_c$, and the bottom panel plots the lapse rate change against the unemployment change, $(\Delta Unemp\, 06-09)_c$. The counties are sorted into 20 equal-sized bins based on the value of the economic variable on the horizontal axis. The blue dots are plotted at the equal-weighted averages for each bin and the orange dots are plotted at the weighted-averaged for each bin. The average in-force amount in 2006 is used to construct the weights, and the orange marker size indicates the bin-level sum of the weights. The blue lines show the OLS predictions while the orange lines show the weighted least squares (WLS) predictions. All three variables are winsorized at the 2.5% and 97.5% percentiles.

The top panel shows a clear negative relationship between the change in the lapse rate and house price changes, and the bottom panel shows a clear positive relationship between lapse rate changes and changes in the unemployment rate. Counties with more adverse housing and labor market conditions during the Great Financial Crisis experienced larger increases in the lapse rates.

We formalize this relationship by estimating county-level regressions. Table 5 presents the WLS results, which we prefer as the baseline specification. The OLS results are presented in Table A2 in the Appendix. Robust standard errors are reported. In Column (1) of Table 5, the point estimate on house price changes is -0.04 and it is statistically significant at the 5% level. The mean and standard deviation of $\Delta Housing\ Price\, 06-09$ are -7.8% and 12.5%, respectively, so that a one-standard deviation decline in house prices is associated with a

Table 4. **Lapsation Risk Exposures to Lapse Trend and Cycle by Firm**

This table reports the lapsation risk exposures of large life insurers to the two lapsation risk factors. Specifically, we run the following regression:

$$Lapse\,Rate_t^j = \alpha^j + \beta^j_{Trend} Lapse\,Trend_t + \beta^j_{Cycle} Lapse\,Cycle_t + \varepsilon^j_t$$

where the superscript j represents the index for the 30 largest life insurer groups from the S&P Global Market Intelligence database.

Rank	Company Name	Mean Lapse	St. dev. Lapse	Corr. w. Employm.	Exposure to Lapse Trend	Exposure to Lapse Cycle
1	Prudential Financial Inc.	5.20	1.19	-0.39	1.08 (0.11)	0.94 (0.15)
2	Northwestern Mutual	3.74	0.35	-0.29	0.16 (0.05)	0.44 (0.06)
3	AIG	6.18	2.48	-0.06	1.68 (0.57)	1.39 (0.76)
4	Transamerica	7.48	1.18	-0.33	0.65 (0.26)	0.95 (0.34)
5	Lincoln Financial	6.02	1.36	-0.28	1.20 (0.21)	0.85 (0.28)
6	New York Life	5.90	0.75	-0.29	0.69 (0.12)	0.41 (0.16)
7	State Farm	6.36	0.98	-0.35	0.83 (0.09)	0.89 (0.12)
8	Protective	5.52	1.30	-0.05	1.06 (0.31)	0.26 (0.41)
9	Principal Financial Group Inc.	4.50	1.78	-0.45	1.65 (0.16)	1.37 (0.21)
10	MassMutual	4.83	0.76	-0.07	0.50 (0.15)	0.65 (0.19)
11	Legal & General U.S. only	4.75	0.98	-0.35	0.91 (0.11)	0.69 (0.15)
12	Primerica	9.97	1.50	-0.36	1.09 (0.16)	1.54 (0.21)
13	Genworth	5.28	1.23	-0.52	0.13 (0.39)	0.46 (0.51)
14	John Hancock	5.68	0.95	-0.52	0.59 (0.15)	0.98 (0.19)
15	Brighthouse Financial	5.77	1.35	-0.44	1.25 (0.23)	0.63 (0.31)
16	Pacific Life	6.31	1.58	-0.50	0.11 (0.38)	1.80 (0.50)
17	Allstate Corp	8.88	1.77	-0.34	1.50 (0.26)	1.32 (0.34)
18	Equitable Holdings	6.30	1.17	-0.29	1.27 (0.18)	0.25 (0.24)
19	MetLife	5.11	1.06	-0.18	0.98 (0.15)	0.65 (0.20)
20	USAA	2.57	0.34	0.01	0.20 (0.08)	0.22 (0.11)
21	Voya Financial Inc.	5.64	1.57	-0.29	1.41 (0.23)	1.01 (0.31)
22	Guardian	5.28	1.16	-0.34	1.17 (0.14)	0.64 (0.19)
23	Berkshire Hathaway Inc.	9.23	4.19	0.14	1.96 (1.28)	-0.35 (1.69)
24	Great-West U.S. only	6.32	2.36	-0.16	1.94 (0.52)	0.85 (0.70)
25	Sammons Enterprises Inc.	6.22	1.02	-0.28	0.89 (0.20)	0.44 (0.27)
26	KUVARE	6.72	1.76	-0.32	0.93 (0.36)	1.63 (0.48)
27	Zurich	8.25	1.47	-0.42	1.32 (0.19)	1.07 (0.25)
28	Nationwide	5.90	1.31	-0.44	1.10 (0.24)	0.77 (0.32)
29	Ohio National	5.85	0.66	-0.33	0.14 (0.21)	-0.20 (0.28)
30	Penn Mutual	5.29	1.30	-0.43	1.04 (0.21)	1.00 (0.27)

Figure 6. **Lapsation Rate Change vs. County-level Economic Variables**

This figure plots the lapsation change between 2006 and 2009 against the county-level economic variables. The top panel plots the lapsation rate change $((\Delta Lapse\,06-09)_c)$ against the housing price change $((\Delta HousingPrice\,06-09)_c)$ and the bottom panel plots the lapsation rate change $((\Delta Lapse\,06-09)_c)$ against the unemployment change $((\Delta Unemp\,06-09)_c)$. Counties are sorted into 20 equal-size bins based on the economic variable on the X-axis. The blue dots are plotted at the equal-weighted averages for each bin and the orange dots are plotted at the weighted-averaged for each bin. The average in-force amount in 2006 are used as the weights, and the orange marker size indicates the bin-level sum of the weights. The blue lines show the OLS predictions while the orange lines show the WLS predictions.

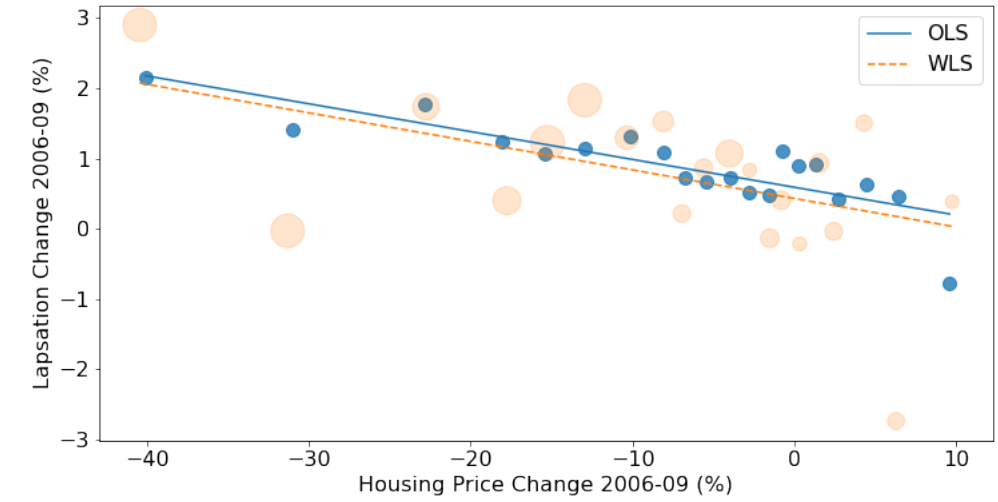

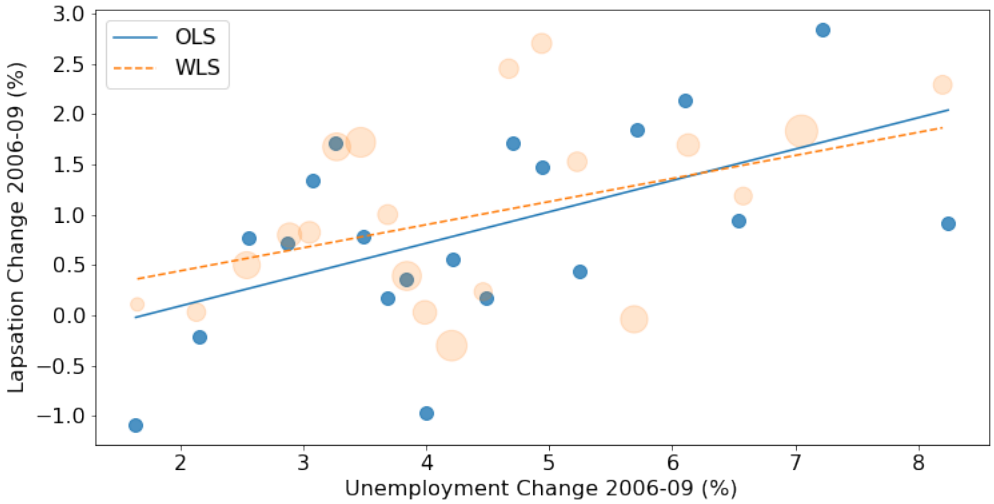

0.51% higher lapsation rate.

Similarly, in Column (4), the coefficient on the unemployment rate change is 0.23 and it is statically significant at the 5% level. The mean and standard deviation of $\Delta Unemp\ Rate\ 06-09$ are 4.4% and 1.7%, respectively, so that a one-standard deviation more severe unemployment rate increase is associated with a 0.39% higher lapsation rate.

In Columns (2) to (3) and (5) to (6), we control for median 2006 income[14] and 2006 log population. The coefficient on house price changes becomes more negative. Larger counties (usually in populous MSAs with higher median income) experienced more severe house price declines, but experienced a smaller increase in lapsation rates. Controlling for income and population thus makes the sensitivity of lapse rates to house prices larger. For unemployment changes, controlling for income and population does not affect the coefficient of interest much.

In Columns (7) to (9), we present the results when both house price changes and unemployment changes are included in the model. The effect from unemployment changes is subsumed by the coefficient on the house price change. The latter is still statistically significant at the 5% level, and is larger in absolute value than in Columns (1) to (3).[15]

In sum, regional variation in economic hardship correlates positively with lapsation rates, adding an additional dimension of heterogeneity to the results from the previous section, and bolstering the evidence that policies tend to lapse more in adverse states of the world.

4 Heterogeneity in Lapse Cycle Exposure Across Policies

For our main results, we study heterogeneity in lapsation risk exposure across individual policies by estimating the Cox proportional hazard model (PHM) specified in Equation (3) on our *Firm Database*.

We first estimate clusters within our sample, using the four ZIP-code level characteristics: income, race, education, and homeownership. Although each of these socioeconomic characteristics is informative on its own, it is likely that there exists an underlying joint distribution among these characteristics. The cluster estimation provides a systematic way to find a representative set of characteristics to summarize the heterogeneity. We implement the K-nearest neighbor (KNN) algorithm with $K = 3$ to estimate the clusters, applied to the

[14] This is the imputed ACS income of 2006. If ACS data exists, we use the data, otherwise we use the predicted income of the following panel regression: $(ACSIncome)_{ct} = \beta * (HUDIncome)_{ct} + \alpha_c + \gamma_t$. The estimated β is ≈ 0.275.

[15] Comparing the WLS results in Table 5 to the OLS results in Table A2, the coefficients are similar in columns (1) to (6). When both house price change and unemployment rate change are included as regressors, the coefficients lose statistical significance, unlike in the WLS.

Table 5. **Lapse Rate Change against County-level Economic Variables: WLS**

This table reports the county-level regression of the change in lapse rates between 2006 and 2009 on the changes in economic variables between 2006 and 2009. We estimate the following cross-sectional regression:

$$(\Delta Lapse06-09)_c = \beta_0 + \beta_1 * (\Delta HousingPrice06-09)_c + \beta_2 * (\Delta Unemp06-09)_c + \gamma * X_c + \varepsilon_c$$

where county c is weighted by the average in-force amount in 2006. Robust standard errors are reported.

	Lapse Chg (1)	Lapse Chg (2)	Lapse Chg (3)	Lapse Chg (4)	Lapse Chg (5)	Lapse Chg (6)	Lapse Chg (7)	Lapse Chg (8)	Lapse Chg (9)
Δ Housing Price 06-09	-0.04058**	-0.04286***	-0.04782***				-0.04188**	-0.05265**	-0.05845**
	(0.01700)	(0.01649)	(0.01641)				(0.02135)	(0.02178)	(0.02271)
Δ Unemp 06-09				0.22959**	0.22791*	0.23695**	-0.01662	-0.11874	-0.12738
				(0.10811)	(0.11869)	(0.11364)	(0.13004)	(0.15784)	(0.15754)
ACS Income 2006		-0.00013	-0.00012		-0.00001	0.00000		-0.00018	-0.00017
		(0.00010)	(0.00010)		(0.00011)	(0.00011)		(0.00013)	(0.00012)
Log Population 2006			-0.00099*			-0.00033			-0.00102*
			(0.00060)			(0.00052)			(0.00061)
Constant	0.00431	0.01170*	0.02344***	-0.00017	0.00034	0.00371	0.00484	0.01820*	0.03073**
	(0.00262)	(0.00645)	(0.00906)	(0.00438)	(0.00966)	(0.01184)	(0.00416)	(0.01055)	(0.01437)
R^2	0.03301	0.03701	0.04198	0.01389	0.01390	0.01456	0.03311	0.03871	0.04395
Adj R^2	0.03174	0.03447	0.03819	0.01269	0.01150	0.01095	0.03055	0.03489	0.03888
N	762	762	762	823	823	823	759	759	759

Standard errors in parentheses

* p<0.1, ** p<0.05, *** p<0.01

standardized variables of log income, *Minority*, *College+*, and *HomeOwnership*, described in Section 2.1.3.[16] See Appendix Table A3 for the estimated cluster centers. We can intuitively label the clusters based on their estimated centers. Cluster 2, the "High Income" cluster has the highest average income (about 155k) among all groups, with high fractions of college graduates and home-ownership and a low fraction of minority households. Among the middle-income population, the KNN estimation distinguishes Cluster 1 and Cluster 3 mainly based on the racial composition. The ZIP codes in Cluster 1 have 54.3% of their population from Black or Hispanic groups, whereas Cluster 3 has only a 14.5% share of minority households, which is similar to Cluster 3. We present our main results using the cluster-based specification, and we refer to Appendix Table A4 for additional results when we include the ZIP-code level characteristics separately in the PHM specification. The signs and the magnitudes of the effects are in line with our main results.

Figure 7 plots the estimated baseline hazard rate function $\lambda_0(n)$, which describes the lapsation rate of a group that has the average covariate values for every characteristic as a function of policy age. The downward-sloping pattern has been documented in industry reports as well (Society of Actuaries and LIMRA, 2019).[17]

Table 6 presents the results using the policy-level data. The first column indicates the policy or policyholder characteristic that we examine. For the attained age of the policyholder, the policy size (death benefit amount in 2016 USD), and the ZIP-code socioeconomic characteristics (income, race, education, homeonwhersip) of the policyholder, we divide the sample into groups and use the group indicator variables. We omit the 40-49 year-old policyholder, the \$200-400k policy size, and the ZIP-code in the middle-income and low-minority cluster (Cluster 3). We include female, smoker, and whole life indicators, and omit the standard risk class. Hence, the reference policy is for a 40-49 year-old male policyholder with a term life policy of \$200-400k who lives in a ZIP code in the middle-income and low-minority cluster (Cluster 3), is a non-smoker, and has average health risk.[18] The data have substantial mass for this combination of characteristics, which is why we chose it as the reference point. The Shock Year variable is an indicator variable that takes on the value of one for a

[16] We use 100 random initial starting points for the iterative algorithm used for estimation. The cluster estimation is robust to the choice of the random seed, given the size of the dataset and the number of initial starting points. The "elbow graph" of the KNN estimation suggests that $K = 3$ is a reasonable choice.

[17] There is a "kink" at the 2-year data point. This results from the operation of the *Firm Database*, which records the status update date for lapsation or surrender, not the last date of coverage. In practice, there is usually a 30-day grace period to declare the lapsation and an additional administrative delay of one to two months. With this limitation, many of "lapses" at the end of the first year are shifted by a few months and measured as the second-year lapse. Because this effect is common to all policies, the effect on the heterogeneous risk exposure β is minimal.

[18] The Risk Class (Better) variable indicates the initial risk classification of the policyholder by the life insurer at the time of underwriting, where the ultra preferred class takes the value +2, the select preferred class takes the value +1, the standard class equals 0, and the substandard class takes the value -1, within either Tobacco or Non-Tobacco risk ratings.

term policy in the year of maturity, allowing us to capture the large spike in lapsation due to the renewability feature common in the U.S. term policy market.[19] Each of the covariates is interacted with the *Lapse Cycle* variable. Columns two and three report point estimates for the PHM coefficients β and associated t-statistics based on the full sample of term and whole life policies; they are our main results. Columns four and five study a subsample estimation on term life policies and the last two columns study whole life policies separately.

Figure 7. **The Estimated Baseline Hazard Rate**

This figure plots the estimated baseline hazard rate from the Cox proportional hazard rate model using the Firm Database. The Cox proportional hazard model specifies that for policy j in the Firm Database issued at time t: $\lambda_{j,t}^{(n)} = \lambda_0(n)\exp(\boldsymbol{\beta}'\boldsymbol{Z}_{j,t+n})$ where $\lambda_0(n)$ is the baseline hazard rate at policy age $n \geq 1$, and the log relative risk is linear in the vector of the policy or policyholder characteristics $\boldsymbol{Z}_{j,t+n}$.

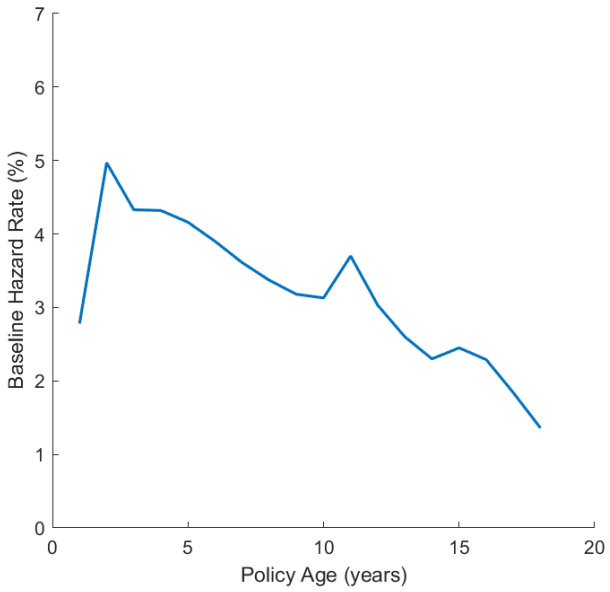

Before we discuss the heterogeneity in lapse cycle exposures, which is our main focus, we discuss the estimated uninteracted lapse rate coefficients. Younger policyholders lapse much more than the reference group, for both term and whole life policies. Older policyholders also lapse more but that effect is weaker and solely driven by term life policies. For whole life, lapsation rates are monotonically declining in age. Female policyholders lapse less. Lapsation is highest for the reference policy size of \$200-400k. Smaller term and whole life

[19] See Figure 33 of Society of Actuaries and LIMRA (2019) for the effect of the shock year lapse "spikes". Both Society of Actuaries (2010) and Milliman (2020) provide detailed discussion on the shock-year lapse effects. Instead of flagging both year T and year $T+1$ as in other source, we only flag year $T+1$ as the shock lapse year, because the *Firm Database* only records the policy status updates dates with about a 3-month delay. This is the same effect that we discuss in the baseline hazard rate graph.

Table 6. **Lapsation Risk Exposures by Policy and Policyholder Characteristics**

This table reports the heterogeneous lapsation risk exposures of life insurance policies depending on various policy or policyholder characteristics. We estimate the following Cox proportional hazard model for policy j in the Firm Database issued at time t:

$$\lambda_{j,t}^{(n)} = \lambda_0(n) \exp(\boldsymbol{\beta}' \boldsymbol{Z}_{j,t+n}),$$

where $\lambda_0(n)$ is the baseline hazard rate at policy age $n \geq 1$, and the log relative risk is linear in the vector of the policy or policyholder characteristics $\boldsymbol{Z}_{j,t+n}$.

Policies included in estimation:	**Term and whole life**		**Term only**		**Whole only**	
	β	t-stat	β	t-stat	β	t-stat
Age Group 00-29	0.40	43.36	0.51	32.42	0.28	24.71
Age Group 30-39	0.13	23.46	0.07	9.05	0.21	25.94
Age Group 50-59	0.09	15.99	0.18	21.06	-0.05	-6.92
Age Group 60 or higher	0.02	3.52	0.42	33.39	-0.26	-31.32
Age Group 00-29 x LapseCycle	-0.02	-1.42	-0.10	-3.94	0.09	5.28
Age Group 30-39 x LapseCycle	-0.01	-1.69	-0.04	-2.99	0.05	4.21
Age Group 50-59 x LapseCycle	-0.15	-16.06	-0.13	-8.50	-0.13	-10.21
Age Group 60 or higher x LapseCycle	-0.29	-24.64	-0.24	-10.53	-0.19	-13.91
Lapse Cycle	0.10	8.29	0.10	5.52	0.26	17.64
Female	-0.02	-4.63	-0.02	-2.95	0.02	2.52
Female x LapseCycle	-0.01	-0.84	-0.02	-1.50	-0.01	-0.78
Size less than 200k	-0.05	-5.46	-0.02	-1.07	-0.08	-7.78
Size 400k to 750k	-0.04	-5.58	-0.01	-0.99	-0.03	-3.21
Size 750k or higher	-0.03	-5.00	0.00	0.29	-0.01	-1.35
Size less than 200k x LapseCycle	-0.05	-3.11	0.01	0.35	-0.06	-3.47
Size 400k to 750k x LapseCycle	-0.01	-0.56	-0.01	-0.55	-0.01	-0.88
Size 750k or higher x LapseCycle	0.02	2.31	-0.01	-0.67	0.07	5.50
Smoker	0.48	65.81	0.51	46.21	0.41	42.51
Smoker x LapseCycle	0.02	1.40	0.03	1.79	0.00	0.03
Risk Class (Better)	-0.22	-97.82	-0.24	-69.08	-0.20	-65.79
Risk Class (Better) x LapseCycle	-0.04	-9.23	-0.01	-2.11	-0.07	-13.71
Cluster 1 (Mid-income, High Minority)	0.22	39.60	0.22	26.73	0.19	26.26
Cluster 2 (High-income)	-0.14	-31.01	-0.14	-19.28	-0.16	-26.03
Cluster 1 x LapseCycle	0.06	6.78	0.08	5.52	0.05	4.04
Cluster 2 x LapseCycle	-0.03	-4.17	-0.06	-5.05	0.01	0.75
Whole & Others	-0.15	-34.43				
Whole & Others x LapseCycle	0.20	27.55				
Shock Year	1.94	98.59	1.92	80.19		
Shock Year x LapseCycle	-1.04	-28.18	-1.08	-24.29		
Number of Subjects	845,026		845,026		845,026	
Number of Periods	6,301,978		6,301,978		6,301,978	

policies lapse substantially less than the reference policy, while the effects for large policies are more similar to the reference group. Smokers lapse much more, and better risk-class (healthier) policyholders lapse significantly less. Policyholders in the high-minority cluster (Cluster 1) lapse substantially more and policyholders in the high-income cluster (Cluster 2) lapse substantially less. The effects are strong and highly significant for both term and whole life policies. Whole life policies see lower average lapsation rates than term life policies. Finally, we observe the spikes in term life lapsation around policy maturity. These effects are broadly consistent with the patterns found in the industry lapse experience (see Society of Actuaries and LIMRA, 2019; Milliman, 2020).

Our main findings uncover large heterogeneity in the exposure of different policies and policyholders to the aggregate lapse cycle. The cyclicality of the reference group can be read off the "Lapse Cycle" coefficient, which is 0.10 for term life and 0.26 for whole life policies, both of which are highly significant. The cyclicality of term life lapsation is a new finding to the literature, which has focused on whole life. The coefficient on "Whole x LapseCycle" in the second column confirms that whole life policies display more cyclical lapsation than term life policies.

Next, we look at heterogeneity by policyholder attained age. For whole life policies, the exposure to the lapse cycle goes up substantially for the young, and is lower for the old, compared to the reference group of 40-49 year olds. For term life, the cyclicality is highest for the reference group, a feature that the full sample inherits.

In terms of policy size, larger (smaller) whole life policies are more (less) sensitive to the lapse cycle. Larger whole life policies have larger cash surrender values, making them more valuable in a recession-induced emergency. For term life policies, there is not much of an effect along the policy size dimension.

Policyholders with higher health risk (negative risk class) have significantly higher lapsation, both among term and whole life policies. For smokers and non-smokers there is no differential sensitivity. The same is true for males versus females.

Policyholders living in the high-minority cluster experience significantly stronger increases in lapsation in recessions, whereas policyholders living in the high-income cluster experience significantly decreases in lapsation in recessions. For Cluster 1 (middle-income, high-minority), both term and whole life policies experience significant increases during the recession. For Cluster 2 (high-income) the effect is mainly concentrated in term life policies. This makes sense as whole life policies are more prevalent among the wealthy, while the opposite is true for term life. The results for term life highlight the importance of binding financial constraints in recessions for term life policyholders, forcing some of them to forfeit their life insurance coverage.

This rich pattern of heterogeneity in exposures suggests that there are important distri-

butional consequences from aggregate lapsation risk. The fact that policyholders with lower health living in lower-income or high-minority ZIP codes are more likely to lapse their policy during economic downturns provides a new perspective on the costs of business cycles. This is particularly relevant if households who lapse their policies are less likely to purchase a new policy in the future.

It also has important implications for pricing if life insurers ignore aggregate lapsation risk when setting premiums. We return to those implications in Section 5.7. We do so for four types of policies: the reference group, high-risk smokers, Cluster 1 containing ZIP codes with a high share of middle-income and minority households, and Cluster 2 containing ZIP codes with a high share of high-income households. Table 7 reports the ratio of the (log) lapse rate in recessions (when the variable *Lapse Cycle* is one standard deviation above its mean of zero) to the average lapse rate (when *Lapse Cycle* is at is mean of zero) minus one. For the reference policy in Panel A, the lapsation rate is 6.0% higher in recessions in the full sample. For whole life policies, lapsation is 16.4% higher in recessions. As Panel B shows, high-risk smokers have higher exposure to the lapse cycle, with lapsation rates that are 9.2% higher in the full sample (21.2% for whole life). Panel C shows that households that live in ZIP codes with high shares of middle-income and minority households (Cluster 1) also display excess sensitivity to the cycle with lapsation rates that are 9.8% higher for the full samaple (19.7% for whole life). Finally, Panel D shows that households that live in ZIP codes with high-income (Cluster 2) see a 4.0% higher lapse sensitivity for the full sample of policies, which is lower than the reference policy. We study these four policies in Section 5.7.

5 Valuation Model

In this section, we develop an asset pricing model to quantify the impact of aggregate lapsation risk on the valuation of life insurance policies. We calibrate the model to be consistent with asset pricing and lapsation data. We then use the model to compute the mispricing and its impact on insurers' profitability when insurance companies do not account for systematic lapsation risk in calculating insurance premiums.

5.1 Summary of the Economic Intuition

Before explaining the details of the model, we discuss the basic economic intuition for how aggregate lapsation risk affects the valuation of life insurance policies.

We denote the probability that a policyholder lapses her policy in the subsequent period by $\lambda_t = \mathbb{E}_t[Lapse_{t+1}]$, where $Lapse_{t+1}$ is one in case of lapsation and zero otherwise. In the presence of aggregate risk, the probability to be used in valuation accounts for the stochastic

Table 7: Heterogeneity in exposure to the lapse cycle

Policies included in estimation:	Term and whole life	Term only	Whole life only
Policy considered:	Term	Term	Whole
Reference policy lapse cycle exposure	0.100	0.103	0.262
	Panel A: Reference policy and policyholder		
(log) lapse rate (LC=0)	6.3%	6.5%	4.8%
(log) lapse rate (LC=0.58)	6.7%	6.9%	5.6%
% diff	6.0%	6.2%	16.4%
	Panel B: High-risk smoker		
(log) lapse rate (LC=0)	12.8%	13.8%	9.0%
(log) lapse rate (LC=0.58)	13.9%	15.1%	10.9%
% diff	9.2%	9.0%	21.2%
	Panel C: High-minority (& Middle-income)		
(log) lapse rate (LC=0)	7.9%	8.1%	5.9%
(log) lapse rate (LC=0.58)	8.6%	9.0%	7.0%
% diff	9.8%	11.0%	19.7%
	Panel D: High-income		
(log) lapse rate (LC=0)	5.5%	5.7%	4.1%
(log) lapse rate (LC=0.58)	5.7%	5.8%	4.8%
% diff	4.0%	2.4%	16.9%

discount factor, $M^{\$}_{t+1}$:

$$\lambda^{Q}_{t} = \mathbb{E}_t \left[\frac{M^{\$}_{t+1}}{\mathbb{E}_t[M^{\$}_{t+1}]} Lapse_{t+1} \right] = \lambda_t + Cov_t \left(\frac{M^{\$}_{t+1}}{\mathbb{E}_t[M^{\$}_{t+1}]}, Lapse_{t+1} \right).$$

We have seen that lapsation is high during economic downturns when investors' marginal utility is high as well. The covariance term is therefore positive and the effective lapsation rate to be used in valuing insurance policies, λ^{Q}, exceeds the actual lapsation rate, λ.

If aggregate lapsation risk is ignored in valuation, the lapsation rate used is too low. This has two opposing effects on the premium charged to policyholders. First, insurance companies pay a commission to insurance brokers to sell their products. If insurers use a lapsation rate that is too low, they understate the probability that the policy lapses before they have been able to recover the fixed cost of selling the policy. As a result, the premium charged is too low.

The opposing effect is a consequence of the fact that insurers charge a fixed insurance premium during the term of the contract, while mortality rates increase. This implies that the first years of the contract are profitable (the premium exceeds the costs of the mortality cover), and the later years of the contract are unprofitable (the premium is lower than the costs of the mortality cover). If insurers use a lapsation rate that is too low, they put too much weight on the second part of the contract, and charge a premium that is too high.

A priori, it is unclear which effect dominates and how large these effects are, how they vary with the markup charged by the insurer, and with macroeconomic conditions such as the low-rate environment. To answer these questions, we develop a quantitative model in the remainder of this section.

5.2 Model Setup

The model builds on the affine valuation models that are widely used in finance. We extend it to value life insurance policies in the presence of aggregate lapsation risk.

We assume that the $N \times 1$ vector of state variables, z_t, follows a Gaussian first-order VAR:

$$z_t = \mu + \Psi z_{t-1} + \Sigma^{\frac{1}{2}} \varepsilon_t, \tag{4}$$

with shocks $\varepsilon_t \sim i.i.d.\mathcal{N}(0, I)$ whose variance is the identity matrix, I. The companion matrix Ψ is an $N \times N$ matrix and $\Sigma^{\frac{1}{2}}$ is a lower-triangular matrix. As detailed below, the state vector contains a one-year government bond yield, the return on a credit portfolio, and the credit spread.

The nominal SDF $M^{\$}_{t+1} = \exp(m^{\$}_{t+1})$ is conditionally log-normal:

$$m^{\$}_{t+1} \;=\; -y^{\$}_{t,1} - \frac{1}{2}\Lambda_t'\Lambda_t - \Lambda_t'\varepsilon_{t+1}. \tag{5}$$

Note that $y^{\$}_{t,1} = -\mathbb{E}_t[m^{\$}_{t+1}] - 0.5\mathbb{V}_t[m^{\$}_{t+1}]$. The risk prices, Λ_t, are assumed to be affine in the state vector, $\Lambda_t = \Lambda_0 + \Lambda_1 z_t$. We impose further restrictions on Λ_0 and Λ_1 below.

All lapsation rates λ are converted to log lapsation rates $\tilde{\lambda}$ satisfying $\exp(-\tilde{\lambda}) = 1 - \lambda$. The log lapsation rate of a policy of age n is modeled as

$$\tilde{\lambda}^{(n)}_t = b^{(n)} \tilde{l}_t,$$

with $b^{(n)} > 0$ and $b'^{(n)} < 0$. We parameterize the term structure of log lapsation rates using a sequence of exposures, $b^{(n)}$, that capture the exposure to a common lapsation factor, $\tilde{l}_t$, that is affine in the state vector, $\tilde{l}_t = a_0 + a_1' z_t$.[20]

[20]While the lapsation rate can in theory become negative, the probability of this happening is so small that

5.3 Nominal Bonds

The model provides a closed-form solution for nominal bond prices, which we summarize in the next proposition.

Proposition 1. Nominal bond yields are affine in the state vector:

$$y_t^{\$}(\tau) = -\frac{A_\tau^{\$}}{\tau} - \frac{B_\tau^{\$\prime}}{\tau} z_t,$$

where the coefficients $A_\tau^{\$}$ and $B_\tau^{\$}$ satisfy the following recursions, with $A_0^{\$} = 0$ and $B_0^{\$} = 0$,

$$A_{\tau+1}^{\$} = A_\tau^{\$} + \frac{1}{2}\left(B_\tau^{\$}\right)' \Sigma \left(B_\tau^{\$}\right) + \left(B_\tau^{\$}\right)' \left(\mu - \Sigma^{\frac{1}{2}} \Lambda_0\right) \tag{6}$$

$$\left(B_{\tau+1}^{\$}\right)' = \left(B_\tau^{\$}\right)' \Psi - e_{yn}' - \left(B_\tau^{\$}\right)' \Sigma^{\frac{1}{2}} \Lambda_1. \tag{7}$$

Proof. See Appendix Section A.1. □

5.4 Term Life Policy

We now use the model to value term life policies. We consider a $T-$year term life insurance contract that is issued at time t. The annual mortality rate at age a is π_a. The life insurance contract is sold via brokers, who receive a multiple κ of the annual premium p as compensation, $C = \kappa p$.

For $\tau = 1, 2, \cdots, T$, the lapse rates $\lambda_{t+\tau}^{(\tau)}$ and the SDF $M_{t+\tau}^{\$}$ are modeled in Section 5.2. We denote the cumulative SDF by $M_{t,1:\tau}^{\$} = \prod_{s=1}^{\tau} M_{t+s}^{\$}$. The valuation equation for the insurance premium equates the present value of premiums to the cost of brokers and the present value of the death benefit,

$$\begin{aligned} & p\mathbb{E}_t\left[1 + \sum_{\tau=1}^{T-1} M_{t,1:\tau}^{\$} \prod_{s=1}^{\tau}(1-\pi_{a+s-1}) \prod_{s=1}^{\tau}(1-\lambda_{t+s}^{(s)})\right] \\ & = C + (1+\phi)\mathbb{E}_t\left[\sum_{\tau=1}^{T} M_{t,1:\tau}^{\$} \pi_{a+\tau-1} \prod_{s=1}^{\tau-1}(1-\pi_{a+s-1}) \prod_{s=1}^{\tau-1}(1-\lambda_{t+s}^{(s)})\right], \end{aligned}$$

where ϕ denotes the markup of the insurance policy before considering the brokerage fee.[21]

we favor this specification that yields simple closed-form solutions over more complicated alternatives.

[21] Note that the timing is such that we first draw the health outcome (survival or death) and then proceed to the lapse decision. If this is reverse, the last term on the right-hand side would have $\prod_{s=1}^{t}(1-\lambda_s)$ instead of $\prod_{s=1}^{t-1}(1-\lambda_s)$.

Using $C = \kappa p$, we can solve for the insurance premium,

$$p = (1+\phi)\frac{\sum_{\tau=1}^{T} \mathbb{E}_t\left[M^{\$}_{t,1:\tau}\prod_{s=1}^{\tau-1}(1-\lambda^{(s)}_{t+s})\right]\mathbb{E}_t\left[\pi_{a+\tau-1}\prod_{s=1}^{\tau-1}(1-\pi_{a+s-1})\right]}{1+\sum_{\tau=1}^{T-1}\mathbb{E}_t\left[M^{\$}_{t,1:\tau}\prod_{s=1}^{\tau}(1-\lambda^{(s)}_{t+s})\right]\mathbb{E}_t\left[\prod_{s=1}^{\tau}(1-\pi_{a+s-1})\right]-\kappa}. \tag{8}$$

Given the assumptions made, we can derive closed-form solutions for $\mathbb{E}_t\left[M^{\$}_{t,1:\tau}\prod_{s=1}^{\tau}(1-\lambda^{(s)}_{t+s})\right]$, which is the key term in computing the insurance premium. The resulting expressions are spelled out in Appendix Section A.2.

5.5 Calibration

We calibrate the model using financial market data at an annual frequency. Instead of directly estimating the VAR model presented in Section 5.2 on annual data, we specify an underlying monthly VAR model. We estimate the monthly model, properly time-aggregated to match moments obtained from annual financial market data. The advantage of this modeling and calibration approach is that it allows us to simultaneously capture the dependency of the lapse rates on the average of financial market state variables during the year and the relationship between the credit risk premium and the credit spread at the end of the year.[22]

The three-dimensional state vector $z_t = (r_t, cr_t, s_t)'$ contains the 1-year Constant Maturity U.S. Treasury rate (GS1 in FRED), the monthly credit return calculated from the ICE BofA BBB US Corporate Index Total Return Index (BAMLCC0A4BBBTRIV in FRED), and the credit spread, which is defined as Moody's Seasoned Baa corporate bond yield relative to the yield on the 10-Year constant-maturity Treasury bond (BAA10Y in FRED) for the sample period 1990–2020. The monthly specification is the same as Equation (4) with the monthly VAR parameters $(\mu, \Psi, \Sigma^{\frac{1}{2}})$:

$$z_t = \mu + \Psi z_{t-1} + \Sigma^{\frac{1}{2}}\varepsilon_t, \tag{9}$$

The monthly dynamics imply the following annual dynamics:

$$z_{t+k} = \left(\sum_{i=0}^{k-1}\Psi^i\right)\mu + \Psi^k z_t + \sum_{i=0}^{k-1}\Psi^i\Sigma^{\frac{1}{2}}\varepsilon_{t+k-i}, \tag{10}$$

[22] Lapsation rate data are available only at an annual frequency. When we model and estimate (in Table 3) the relationship between the annual lapse rates and the financial market state variables, the lapse rate depends on the average state variables throughout the year not just on the end-of-year state variables. Using a monthly VAR allows us to model the annual lapse rate as a function of the 12-month average of monthly state variables.

and

$$\sum_{k=1}^{K} z_{t+k} = \sum_{k=1}^{K} \left(\sum_{i=0}^{k-1} \Psi^i \right) \mu + \sum_{k=1}^{K} \Psi^k z_t + \sum_{k=1}^{K} \sum_{i=0}^{k-1} \Psi^i \Sigma^{\frac{1}{2}} \varepsilon_{t+k-i}. \tag{11}$$

Equation (10) describes the dynamics of the annually-sampled interest rate and the credit spread (r_{t+12} and s_{t+12}). Equation (11) describes the annual log holding period return on the credit portfolio, which is the sum of twelve monthly log returns ($\sum_{k=1}^{12} cr_{t+k}$). Equation (11) multiplied by $1/12$ also describes the dynamics of the state variables that are averaged over the year. It is those averages that explain the lapsation behavior.

The monthly nominal SDF $M_{t+1}^{\$} = \exp(m_{t+1}^{\$})$ is given by:

$$m_{t+1}^{\$} = -\frac{\delta_0}{12} - \frac{\delta_1' z_t}{12} - \frac{1}{2}\Lambda_t'\Lambda_t - \Lambda_t' \varepsilon_{t+1}, \tag{12}$$

where the one-month discount rate $y_{t,1}^{\$} = \dfrac{\delta_0}{12} + \dfrac{\delta_1' z_t}{12}$ is an affine function of the state variable z_t. We parameterize the market price of risk Λ_t as:

$$\Lambda_t = \Lambda_0 + \Lambda_1 z_t = \Lambda_0 + \hat{\Lambda}_1 e_3' z_t,$$

with two prices of risk in $\Lambda_0 = (\Lambda_0^r, \Lambda_0^{cr}, 0)'$ and one in $\hat{\Lambda}_1 = (0, \zeta, 0)'$. This implies that interest rate risk and credit risk are priced and that the variation in risk prices is driven by the credit spread.

We use the following three moments to calibrate these three parameters. First, we match the average slope of the yield curve, defined as the difference between the 10- and 1-year Treasury bond yields. Second, we match the unconditional credit risk premium. Third, we match the linear dependence of the credit risk premium on the lagged credit spread. Additionally, (δ_0, δ_1) are estimated from the restriction that the one-year risk-free interest rate implied by the monthly SDF equals the one-year bond yield included in the state vector, r_t.

We model the monthly excess return on the credit portfolio as:

$$cr_{t+1} - y_{t,1}^{\$} = \gamma_0 + \gamma_1 s_t + \sigma^{cr} e_{t+1},$$

with $e_{t+1} \sim \mathcal{N}(0,1)$, so that the expected excess return depends on the credit spread:

$$E_t[cr_{t+1}] - y_{t,1}^{\$} = \gamma_0 + \gamma_1 s_t.$$

The Euler equation for the credit portfolio then implies:

$$E_t[cr_{t+1}] + \frac{1}{2}V_t[cr_{t+1}] - y^{\$}_{t,1} = -Cov_t[cr_{t+1}, m^{\$}_{t+1}]$$

Using our assumption on the credit return and the affine structure of the SDF, this can be rewritten as:

$$\gamma_0 + \gamma_1 s_t + \frac{1}{2}(\sigma^{cr})^2 = \Lambda^r_0 \sigma^{cr} Cov_t[e_{t+1}, \varepsilon^r_{t+1}] + (\Lambda^{cr}_0 + \zeta s_t)\sigma^{cr} Cov_t[e_{t+1}, \varepsilon^{cr}_{t+1}]$$

Matching the unconditional credit risk premium delivers the second moment condition:

$$\gamma_0 + \gamma_1 E[s_t] + \frac{1}{2}(\sigma^{cr})^2 = \Lambda^r_0 \sigma^{cr} Cov[e_{t+1}, \varepsilon^r_{t+1}] + (\Lambda^{cr}_0 + \zeta E[s_t])\sigma^{cr} Cov[e_{t+1}, \varepsilon^{cr}_{t+1}] \tag{13}$$

and matching the conditional credit spread delivers the third moment condition:

$$\gamma_1 = \zeta \sigma^{cr} Cov[e_{t+1}, \varepsilon^{cr}_{t+1}] \tag{14}$$

Appendix B contains the details of the calibration process. The estimated monthly dynamics that result from matching moments measured in annual data are as follows:

$$\begin{bmatrix} r_{t+1} \\ cr_{t+1} \\ s_{t+1} \end{bmatrix} = \begin{bmatrix} 0.0006 \\ -0.0139 \\ 0.0026 \end{bmatrix} + \begin{bmatrix} 0.9792 & 0 & 0 \\ 0.0933 & 0 & 0.7245 \\ 0 & 0 & 0.8888 \end{bmatrix} \begin{bmatrix} r_t \\ cr_t \\ s_t \end{bmatrix} + \begin{bmatrix} 0.0041 & 0 & 0 \\ 0.0013 & 0.0242 & 0 \\ -0.0023 & -0.0025 & 0.0016 \end{bmatrix} \begin{bmatrix} \varepsilon^r_{t+1} \\ \varepsilon^{cr}_{t+1} \\ \varepsilon^s_{t+1} \end{bmatrix}$$

The estimated market price of risks are $\Lambda^r_0 = -0.1265$, $\Lambda^{cr}_0 = -0.5365$, and $\zeta = 29.98$. The model then matches the unconditional slope of the yield curve of 1.36% and the unconditional credit risk premium of 4.43% (equivalently, the monthly unconditional credit risk premium of 0.41%), as well as the observed dependence of the annual credit risk premium on the 12-month lagged credit spread.

Next, we calibrate the parameters for the aggregate lapsation process, modeled as follows,

$$\tilde{l}_t = a_0 + a_1' \bar{z}_t,$$
$$\tilde{\lambda}^{(n)}_t = b^{(n)} \tilde{l}_t,$$

where $\bar{z}_t$ denotes the 12-month moving average of the state variables. We first calibrate the parameters a_0 and a_1. By regressing the log lapsation rate $\tilde{l}_t$ on a constant, the constant-maturity U.S. Treasury 10-year rate ($y^{\$}_{10,t}$), and the Baa–10-year spread (s_t) over the period 2000 to 2020 (annual average financial market data), we obtain the following relation-

Figure 8. **Lapse Rate Calibration**

This figure plots the calibrated lapse rates from the model and compare it to the Data for 2007-2009 and 2009-2013 periods (Society of Actuaries and LIMRA, 2012, 2019). See Section 5.5 for the details of the calibration process.

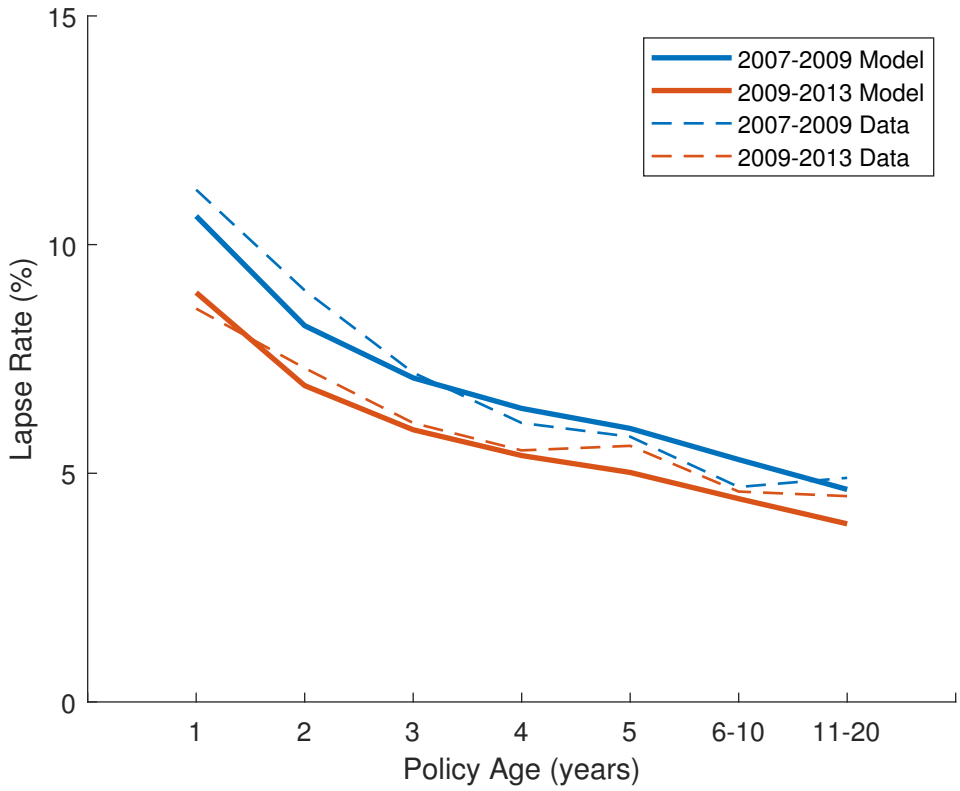

ship: $\tilde{l}_t = 0.0094 + 0.85 y^{\$}_{10,t} + 0.94 s_t$. Using the theoretical relationship $y^{\$}_{10,t} = 0.02986 + 0.41247 r_t$ from the calibrated yield curve, we obtain the coefficients $a_0 = 0.0347$ and $a_1 = (0.35, 0, 0.94)'$.

We calibrate the term structure of lapsation coefficients $\{b^{(n)}\}$ by parameterizing $\{b^{(n)}\} = u + \frac{v}{n+w}$, and we search for the vector (u, v, w) that delivers the closest fit for the 2007-2009 and 2009-2013 lapsation term structures to the term policy lapsation curves observed in the data (Society of Actuaries and LIMRA, 2012, 2019).[23] The calibrated term structure is $b^{(n)} = 0.54 + \frac{1.75}{n+0.75}$ and the model-implied lapsation term structure is reasonably close to the data, as shown in Figure 8.

Figure 9 presents the historical paths of the model state variables, and the model-implied

[23] We do not model the extendibility of a term life policy and the associated "shock lapses" at the end of the level premium periods, so we calculate the 6-10 and 11-20 average lapse rates excluding the policy ages affected by the shock lapses (10, 11, 15, 16, 20). See Society of Actuaries (2010) for a detailed investigation of the shock lapses after the level-premium period. The report shows that most of the shock lapses are occurring at the end of the policy age T and the beginning of the policy age $T + 1$.

Figure 9. **Lapsation Model and Data**

The top panel plots the historical paths of two state variables, (r_t, s_t), of the asset pricing model. The middle panel compares the actual lapse rate data with the model-implied lapse rates. For the details of model calibration, see Section 5.5. The bottom panel plots the model-implied market price of risk.

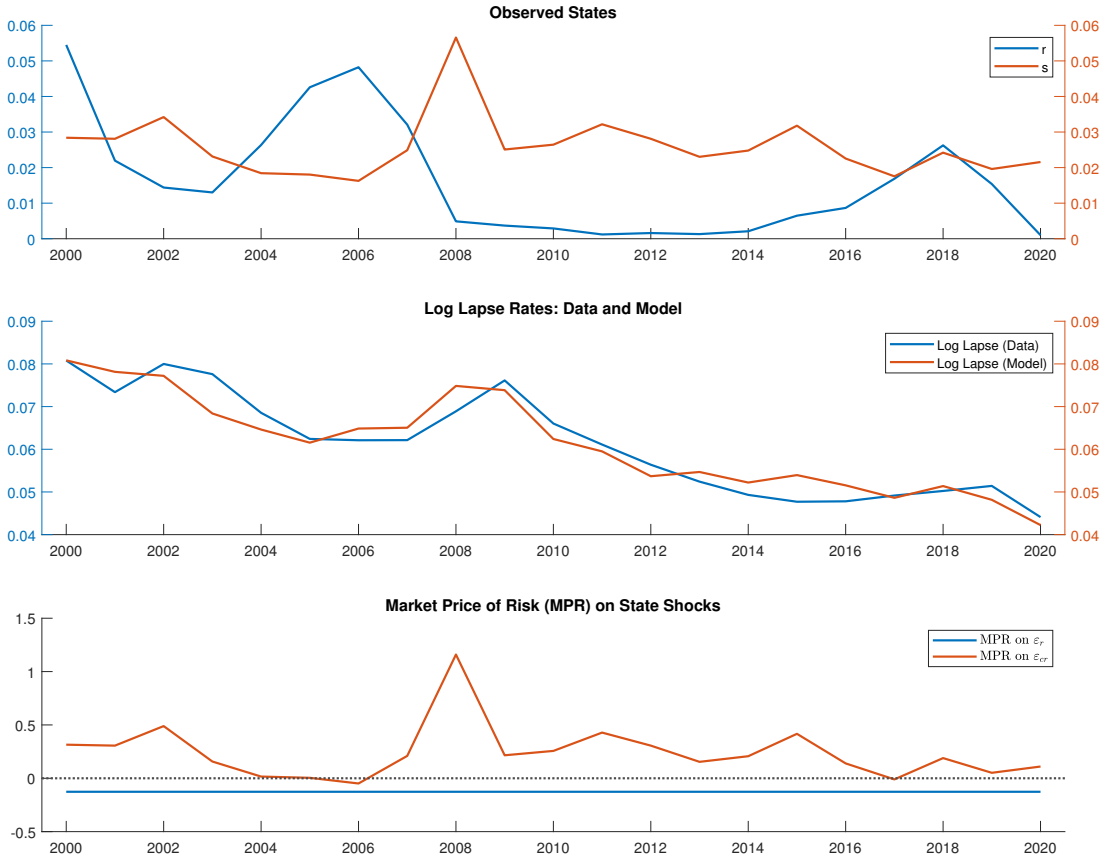

lapse rates and the market price of risks. In the top panel, we plot the first and the third state variables (r_t, s_t) retrieved from FRED between 2000 and 2020. The middle panel compares the actual lapse rate data with the model-implied lapse rates, showing that our lapsation model provides a good fit. The bottom panel shows the time variation in the market price of risk on the credit return shock (the market price of risk on the interest rate shock is constant). During the Great Financial Crisis when the credit spread was high, the market price of credit risk was high, and lapsation was high. It is this positive covariance between lapsation rates and marginal utility that is the key new ingredient in our insurance pricing model.

5.6 Mispricing when Ignoring Aggregate Lapsation Risk

We now study an insurer who does not consider systematic lapsation risk when pricing life insurance contracts. We first consider the correct premium when the life insurer properly

accounts for aggregate lapsation risk. Equation (8) implied that the correct expected profit of the insurer, V, is:

$$
\begin{aligned}
V^{correct} &= p \cdot \Bigg(\underbrace{1 + \sum_{\tau=1}^{T-1} \mathbb{E}_t \left[M^{\$}_{t,1:\tau} \prod_{s=1}^{\tau} (1 - \lambda^{(s)}_{t+s}) \right] \mathbb{E}_t \left[\prod_{s=1}^{\tau} (1 - \pi_{a+s-1}) \right]}_{=\alpha(T)} - \kappa \Bigg) \\
&\quad - \underbrace{\sum_{\tau=1}^{T} \mathbb{E}_t \left[M^{\$}_{t,1:\tau} \prod_{s=1}^{\tau-1} (1 - \lambda^{(s)}_{t+s}) \right] \mathbb{E}_t \left[\pi_{a+\tau-1} \prod_{s=1}^{\tau-1} (1 - \pi_{a+s-1}) \right]}_{=\beta(T)} \\
&= p \cdot (\alpha(T) - \kappa) - \beta(T) \\
&= \phi \beta(T),
\end{aligned}
$$

where we have a closed-form solution for $\alpha(T)$ and $\beta(T)$, see Appendix B.3.

Intuitively, $\alpha(T)$ measures the number of years of premium income the insurer can expect to receive in the presence of lapsation risk and mortality risk. The first arrival of either lapsation or policyholder death ends the premium revenue claim. $\beta(T)$ measures the expected value of a \$1 death benefit. This death benefit only needs to be paid out if the policyholder dies during the term of the life insurance contract and the policy did not yet lapse.

We contrast this case with the case where an insurer ignores the covariance between the SDF and lapsation when pricing the term life insurance contract. To model this scenario, we assume that the lapse rate depends on an independent lapsation factor, which is defined as $\tilde{l}^{ind}_t = a_0 + a_1' \bar{z}^{ind}_t$. The independent state vector z^{ind}_t follows the process $z^{ind}_{t+1} = \mu + \Psi z^{ind}_t + \Sigma^{\frac{1}{2}} \tilde{\varepsilon}_{t+1}$ with shocks $\tilde{\varepsilon}_t \sim N(0, I)$ that are independent from ε_t. This modeling approach preserves the distribution of lapsation rates, but makes lapsation risk independent from financial market risks.

When both $\alpha(T)$ and $\beta(T)$ are incorrectly calculated based on this independent lapsation model, denoted by $\tilde{\alpha}(T)$ and $\tilde{\beta}(T)$, respectively, the premium is set as $\tilde{p} = (1 + \phi) \frac{\tilde{\beta}(T)}{\tilde{\alpha}(T) - \kappa}$. We can calculate $\tilde{\alpha}(T)$ and $\tilde{\beta}(T)$ also in closed form as $\tilde{\alpha}(T) = 1 + \sum_{\tau=1}^{T-1} L_\tau Z_\tau \prod_{s=1}^{\tau-1} (1 - \pi_{a+s-1})$ and $\tilde{\beta}(T) = \sum_{\tau=1}^{T} L_{\tau-1} Z_\tau \pi_{a+\tau-1} \prod_{s=1}^{\tau-1} (1 - \pi_{a+s-1})$ for $Z_\tau = E_t \left[M^{\$}_{t,t+1:t+\tau} \right]$ and $L_\tau = E_t \left[\prod_{s=1}^{\tau} (1 - \lambda^{(s)}_{t+s}) \right]$. Appendix A.2 and Section B.3 contain the affine recursions for L_τ and Z_τ.

When the premium $\tilde{p}$ is charged, but actual lapsation is subject to aggregate risk, the

insurer's profit is given by:

$$\begin{aligned} V^{realized} &= \tilde{p} \cdot (\alpha(T) - \kappa) - \beta(T) \\ &= (1+\phi)\left(\frac{\alpha(T)-\kappa}{\tilde{\alpha}(T)-\kappa}\right)\tilde{\beta}(T) - \beta(T). \end{aligned}$$

We measure the impact of ignoring aggregate priced risk on the life insurer's profits as $Mispricing(\%) = \frac{V^{realized} - V^{correct}}{V^{correct}}$. We first study the numerator of this expression:

$$\begin{aligned} V^{realized} - V^{correct} &= (1+\phi)\left(\frac{\alpha(T)-\kappa}{\tilde{\alpha}(T)-\kappa}\right)\tilde{\beta}(T) - \beta(T) - \phi\beta(T) \\ &= (1+\phi)\left(\frac{\alpha(T)-\kappa}{\tilde{\alpha}(T)-\kappa} - 1\right)\tilde{\beta}(T) + (1+\phi)\left(\tilde{\beta}(T) - \beta(T)\right) \end{aligned}$$

We find that $\alpha(T) < \tilde{\alpha}(T)$ and $\beta(T) < \tilde{\beta}(T)$. Intuitively, lapse rates tend to increase during bad times (high SDF states). Taking this covariance into account shortens the duration of the premium leg and lowers the expected discounted death benefit payment. The effect of aggregate lapsation risk is to increase the effective lapse rates. The risk-neutral lapse rates (under the $\mathbb{Q}$ measure) are higher than the physical lapse rates (under the $\mathbb{P}$ measure).

We use the notation $\tilde{\alpha}(T)/\alpha(T) = 1 + \Delta_{\alpha,T}$ and $\tilde{\beta}(T)/\beta(T) = 1 + \Delta_{\beta,T}$ for $\Delta_{\alpha,T}, \Delta_{\beta,T} > 0$. Then, after dividing the previous expression by $V^{correct}$ and some algebraic manipulation, we can express the Mispricing(%) measure as the sum of two components:

$$\begin{aligned} Mispricing(\%) &= \frac{V^{realized} - V^{correct}}{V^{correct}} \\ &= \underbrace{(1+\phi^{-1})\left(\frac{\Delta_{\alpha,T}}{1+\Delta_{\alpha,T}} - \frac{\Delta_{\alpha,T}}{1+\Delta_{\alpha,T}-\kappa/\alpha(T)}\right)(1+\Delta_{\beta,T})}_{=Fixed-Cost\,Effect<0} \\ &\quad + \underbrace{(1+\phi^{-1})\left(\frac{\Delta_{\beta,T}}{1+\Delta_{\beta,T}} - \frac{\Delta_{\alpha,T}}{1+\Delta_{\alpha,T}}\right)(1+\Delta_{\beta,T})}_{=Mortality\,Effect>0} \end{aligned} \tag{15}$$

The fixed-cost effect term shows how the presence of the broker cost ($\kappa > 0$) affects our mispricing measure. The first term is zero when $\kappa = 0$. The insurer has to pay the fixed cost when the policy is underwritten. Early lapsation means that the insurer may not earn enough premium income to offset the cost of the broker's fee. The higher the lapsation rate, the stronger the detrimental effect of fixed costs on profits. Since the effective lapsation rate is higher when accounting for priced aggregate lapsation risk, the fixed-cost effect is negative.

We label the second effect a mortality effect because the sign of this term is determined by the relative size of $\Delta_{\beta,T}$ and $\Delta_{\alpha,T}$. We observe that $\Delta_{\beta,T} > \Delta_{\alpha,T}$ in our calibration when mortality rates increase with age. With a flat mortality curve, $\Delta_{\alpha,T} \approx \Delta_{\beta,T}$ and mispricing mostly reflects the fixed-cost effect. However, under a realistic mortality curve, the mortality rate exponentially rises in age and $\Delta_{\beta,T} > \Delta_{\alpha,T}$. The mortality effect contributes positively to the mispricing measure. Intuitively, the insurer charges a flat premium throughout the life of the contract. The expected cost, by contrast, increases with age as mortality rates increase. Putting the fixed cost aside, the insurer experiences profits during the early years (as the flat premium exceeds the costs of mortality coverage) and losses during the later years of the contract (as the flat premium is lower than the costs of mortality coverage). If the insurer understates lapsation risk, it puts more weight on the later years during which the insurer experiences losses. As a result, the premium is set too high and the insurers unexpectedly earns excess profits.

Because the mispricing decomposition shows two countervailing effects, we need to quantitatively assess the relative magnitude of the two effects. We do so for a hypothetical 40 year-old male policyholder with a realistic mortality curve.[24] The fee paid to the broker is known to be between 50% to 100% of the first-year premium revenue, so we use $\kappa = 0.5, 0.75$, and 1.0, with a benchmark value of $\kappa = 0.75$. We vary the markup parameter ϕ in a reasonable range by using values $\phi = 0.05$, 0.1, and 0.2. In Appendix C, we test the validity of the markup assumption by calculating the insurer's expected share θ from the underwriting profit, after paying the broker's share $(1 - \theta)$. The 40% to 50% profit share range for term policies ranging from 10 to 20 years in maturity (see Table A1) in our baseline cases $\phi = 10\%$ and $\kappa = 0.75$ is in line with our understanding of the profit sharing arrangement between insurers and brokers in the industry.

Table 8 reports the mispricing measure and its decomposition. We find that the mortality effect dominates the fixed-cost effect, so that insurers who ignore priced aggregate lapsation risk earn excess profits. In our baseline case, $\kappa = 0.75$ and $\phi = 10\%$, the realized profit for a 10-year term policy is 6.9% higher than the theoretically correct one. This mispricing is decomposed into the two effects previously discussed in the second and third panels of the table. The insurer has to pay 75% of the first year premium to compensate brokers. Ignoring the accelerated lapsation during recessions (higher lapsation under $\mathbb{Q}$) results in 3.2% understatement of the profit. On the other hand, the insurer charges a higher premium than the theoretically correct one (0.6% higher premium before markup and fixed-costs), as she prices a higher likelihood of having to pay out the death benefit when she assumes that

[24] We use the 2017 Loaded CSO (Commissioners Standard Ordinary) Composite mortality table (https://www.soa.org/resources/experience-studies/2015/2017-cso-tables). We use the select mortality table to reflect the fact that insurers in practice are able to select policyholders with lower-than-population mortality risk, at least in the early years of the policy.

lapsation rates are lower (under $\mathbb{P}$ than under $\mathbb{Q}$). The mortality effect raises the expected profit by 10.0%. Since the mortality effect outweighs the fixed-cost effect, ignoring systematic lapsation risk in pricing decisions results in an excess profit of 6.9% compared to the case where the insurer correctly considered systematic lapsation risk. Term life policies would be cheaper in the world with correct pricing and profits would be lower.

The mispricing effect increases strongly in the maturity of the policy. The excess profit is 29.3% for a 20-year policy, due to a much stronger mortality effect. The reason is that mortality rises exponentially in age, and is much higher around age 60 than around age 40. This backloading of mortality risk interacts with lapsation risk. Understating lapsation risk in the incorrect pricing model results in a much higher expected death benefit payout than in the correct pricing model. The incorrect insurer charges a much higher premium and earns much higher profits. We have verified that with a (counter-factually) flat mortality rate profile, the mortality effect remains near zero for the 20-year policy.

Mispricing falls in both κ and ϕ. A higher fixed cost κ, while holding the markup ϕ fixed, results in a lower fixed-cost effect while the mortality effect is not changed. As the markup ϕ increases, holding κ fixed, both the fixed-cost effect and the mortality effect decline due to the $1 + \phi^{-1}$ term in Equation (15).

5.7 Cross-Sectional Variation in Mispricing

We now explore how heterogeneity in exposure to aggregate risk affects the pricing of premiums and insurers' profits when insurers ignore aggregate risk in pricing. We use the results from Table 6. We do so for the four types of policies discussed in Table 7: the reference group, high-risk smokers, the high-minority ZIP code residents (Cluster 1), and the high-income ZIP code residents (Cluster 2).

We first map the results from the proportional hazard model to the affine model. To do so, we adjust a_0 and $a_1(3)$ so that the ratio of log lapse rates in the affine model matches the ratio in the hazard model, where the numerator is the log lapse rate of the policy type under consideration and the denominator the log lapse rate in the average policy.[25] We compute this ratio when the lapse cycle is zero (its unconditional mean) and when it is equal to one standard deviation (measured as a percentage deviation, as shown in Table 7). This gives us two moments to calibrate a_0 and $a_1(3)$ for each type of policy.

The top panel of Figure 10 reports the lapse rates when the lapse cycle equals zero and when it is equal to one standard deviation. In the middle panel, we plot the impact on the premium mispricing, and in the bottom panel we plot the impact on insurers' profits. We

[25]For the average policy, we calculate the mean values of each uninteracted covariate and use the mean values to calculate the lapse cycle exposure.

Table 8. **Mispricing of Term Life Policies without Aggregate Lapse Risk**

This table presents the calculated mispricing measure defined in Section 5.6 by

$$Mispricing(\%) = \frac{V^{realized} - V^{correct}}{V^{correct}}$$

where $V^{correct} = \phi\beta(T)$ is the correct profit of selling the term policy at markup ϕ assuming the correct pricing, and $V^{realized} = \tilde{p} \cdot (\alpha(T) - \kappa) - \beta(T)$ is the realized valuation based on the incorrect pricing when the aggregate lapsation risk is ignored.

Mispricing (%)				
		κ=0.5	κ=0.75	κ=1.0
10-year Term Policy	ϕ= 5%	15.3%	13.1%	10.7%
	ϕ= 10%	8.0%	6.9%	5.6%
	ϕ= 20%	4.4%	3.7%	3.1%
15-year Term Policy	ϕ= 5%	34.3%	31.6%	28.8%
	ϕ= 10%	18.0%	16.6%	15.1%
	ϕ= 20%	9.8%	9.0%	8.2%
20-year Term Policy	ϕ= 5%	59.0%	56.0%	52.8%
	ϕ= 10%	30.9%	29.3%	27.7%
	ϕ= 20%	16.9%	16.0%	15.1%
Fixed-Cost Effect (%)				
		κ=0.5	κ=0.75	κ=1.0
10-year Term Policy	ϕ= 5%	-3.9%	-6.0%	-8.4%
	ϕ= 10%	-2.0%	-3.2%	-4.4%
	ϕ= 20%	-1.1%	-1.7%	-2.4%
15-year Term Policy	ϕ= 5%	-4.8%	-7.4%	-10.3%
	ϕ= 10%	-2.5%	-3.9%	-5.4%
	ϕ= 20%	-1.4%	-2.1%	-2.9%
20-year Term Policy	ϕ= 5%	-5.5%	-8.5%	-11.7%
	ϕ= 10%	-2.9%	-4.5%	-6.1%
	ϕ= 20%	-1.6%	-2.4%	-3.3%
Mortality Effect (%)				
		κ=0.5	κ=0.75	κ=1.0
10-year Term Policy	ϕ= 5%	19.1%	19.1%	19.1%
	ϕ= 10%	10.0%	10.0%	10.0%
	ϕ= 20%	5.5%	5.5%	5.5%
15-year Term Policy	ϕ= 5%	39.1%	39.1%	39.1%
	ϕ= 10%	20.5%	20.5%	20.5%
	ϕ= 20%	11.2%	11.2%	11.2%
20-year Term Policy	ϕ= 5%	64.5%	64.5%	64.5%
	ϕ= 10%	33.8%	33.8%	33.8%
	ϕ= 20%	18.4%	18.4%	18.4%

decompose the profit effect into the mortality effect and the fixed cost effect. In valuing these various policies, we use group-specific mortality curves.

For high-risk smokers, the lapse rate is both much higher on average and much more sensitive to the cyclical factor. As a result, the premium mispricing is 10.3%, more than two times as large as for the reference policy (4.2% mispricing). The bottom panel shows that high-risk smokers are particularly profitable policies for insurers. Ignoring aggregate lapsation risk results in profits that are 114% too high. We find the same effects on excess premiums and profits, albeit to a smaller degree, for the high-minority cluster (Cluster 1) households. On the other hand, the high-income cluster (Cluster 2) households face lower mispricing both in premium and profit terms.

The key takeaway is that an insurance company charging a fixed markup across policies inadvertently charges heterogeneous markups when ignoring aggregate risk in setting insurance premiums. The implicit markups are particularly high for households living in high-minority ZIP codes, and high-risk households for whom life insurance coverage is particularly valuable. The covariance between policy premiums or policy profits on the one hand and policyholder marginal utility on the other hand is positive. Thus, ignoring lapsation risk (inadvertently) results in "wrong-way-around" redistribution. These cross-sectional pricing effects may affect both the extensive and the intensive margin of coverage.

6 Conclusion

We study aggregate lapsation risk in the life insurance sector. We construct two lapsation risk factors that explain a large fraction of the common variation in lapse rates of the 30 largest life insurance companies. The first is a cyclical factor that is positively correlated with credit spreads and unemployment, while the second factor is a trend factor that correlates with the level of interest rates. Using a novel policy-level database from a large life insurer, we examine the heterogeneity in risk factor exposures based on policy and policyholder characteristics. Young policyholders with higher health risk in lower-income areas are more likely to lapse their policies during economic downturns. We explore the implications for hedging and valuation of life insurance contracts. Ignoring aggregate lapsation risk results in mispricing of life insurance policies. The calibrated model points to overpricing on average and important cross-sectional implications. Young and high-health risk households face higher effective mark-ups than the old and healthy.

Figure 10: **The impact of heterogeneous lapse cycle exposures on premiums and profits**
The top panel reports the log lapse rate when the lapse cycle is equal to zero or to one standard deviation. The middle panel reports premium mispricing, and the bottom panel reports mispricing of insurers' profits. We decompose the total effect from mispricing on profits into the mortality effect and the fixed cost effect.

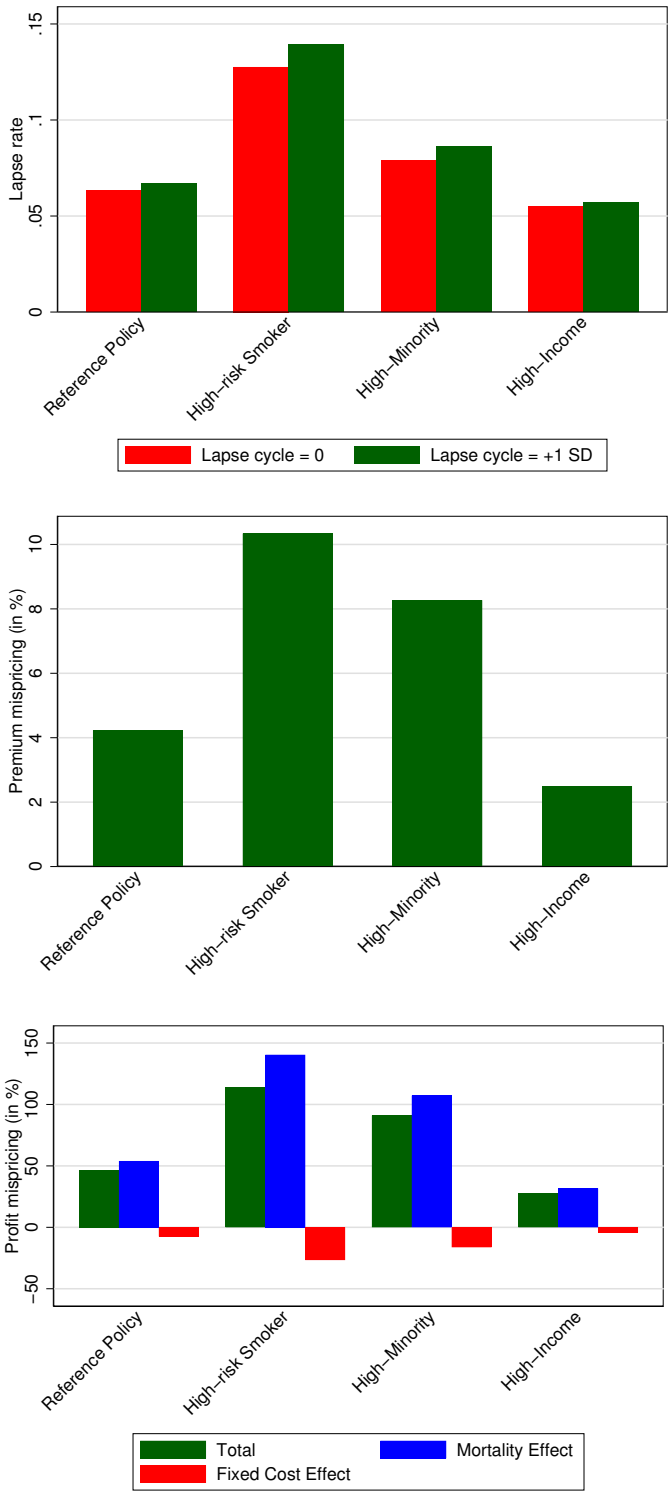

References

Bauer, Daniel, Jin Gao, Thorsten Moenig, Eric R Ulm, and Nan Zhu. 2017. "Policyholder exercise behavior in life insurance: The state of affairs." *North American Actuarial Journal* 21 (4):485–501.

Boyarchenko, Nina, Andreas Fuster, and David O. Lucca. 2019. "Understanding Mortgage Spreads." *Review of Financial Studies* 32 (10):3799–3850.

Chernov, Mikhail, Brett R. Dunn, and Francis A. Longstaff. 2018. "Macroeconomic-Driven Prepayment Risk and the Valuation of Mortgage-Backed Securities." *Review of Financial Studies* 31 (3):1132–1183.

Dar, Atul and C Dodds. 1989. "Interest rates, the emergency fund hypothesis and saving through endowment policies: some empirical evidence for the UK." *Journal of Risk and Insurance* :415–433.

Deng, Yongheng, John M. Quigley, and Robert Van Order. 2000. "Mortgage Terminations, Heterogeneity and the Exercise of Mortgage Options." *Econometrica* 68 (2):275–307.

Diep, Peter, Andrea L. Eisfeldt, and Scott Richardson. 2021. "The Cross Section of MBS Returns." *Journal of Finance* 76 (5):2093–2151.

Eling, Martin and Michael Kochanski. 2013. "Research on lapse in life insurance: what has been done and what needs to be done?" *The Journal of Risk Finance* .

Fang, Hanming and Edward Kung. 2021. "Why do life insurance policyholders lapse? The roles of income, health, and bequest motive shocks." *Journal of Risk and Insurance* 88 (4):937–970.

Fier, Stephen G and Andre P Liebenberg. 2013. "Life insurance lapse behavior." *North American Actuarial Journal* 17 (2):153–167.

Fisher, Jack, Alessandro Gavazza, Lu Liu, Tarun Ramadorai, and Jagdish Tripathy. 2021. "Refinancing Cross-Subsidies in the Mortgage Market." Working Paper.

Gerardi, Kristopher, Paul Willen, and David Hao Zhang. 2021. "Mortgage Prepayment, Race, and Monetary Policy." Working Paper.

Gottlieb, Daniel and Kent Smetters. 2021. "Lapse-Based Insurance." *American Economic Review* 111 (8):2377–2416.

Greenwald, Daniel L., Tim Landvoigt, and Stijn Van Nieuwerburgh. 2021. "Financial Fragility with SAM?" *Journal of Finance* 76 (2):651–706.

Hamilton, James D. 2018. "Why You Should Never Use the Hodrick-Prescott Filter." *The Review of Economics and Statistics* 100 (5):831–843.

Hendel, Igal and Alessandro Lizzeri. 2003. "The Role of Commitment in Dynamic Contracts: Evidence from Life Insurance." *Quarterly Journal of Economics* 118 (1):299–328.

Kiesenbauer, Dieter. 2012. "Main determinants of lapse in the German life insurance industry." *North American Actuarial Journal* 16 (1):52–73.

Kim, Changki. 2005. "Modeling surrender and lapse rates with economic variables." *North American Actuarial Journal* 9 (4):56–70.

Koijen, Ralph and Stijn Van Nieuwerburgh. 2020. "Combining Life and Health Insurance." *Quarterly Journal of Economics* 135 (2):913–958.

Kubitza, Christian, Nicolaus Grochola, and Helmut Grundl. 2022. "Life Insurance Convexity." Working Paper.

Kuo, Weiyu, Chenghsien Tsai, and Wei-Kuang Chen. 2003. "An empirical study on the lapse rate: The cointegration approach." *Journal of Risk and Insurance* 70 (3):489–508.

Linton, M.A. 1932. "Panics and cash Values." *Transactions of the actuarial Society* 33:265–394.

Milliman. 2020. "MIMSA III 2020: Study on Mortality and Lapse Rates in Level Term Life Insurance." Milliman Research Report.

Outreville, J. Francois. 1990. "Whole-life Insurance Lapse Rates and the Emergency Fund Hypothesis." *Insurance: Mathemetaics and Economics* 9:249–255.

Schott, Francis H. 1971. "Disintermediation through policy loans at life insurance companies." *The Journal of finance* 26 (3):719–729.

Schwartz, Eduardo S. and Walter N. Torous. 1989. "Prepayment and the Valuation of Mortgage-Backed Securities." *Journal of Finance* 44 (2):375–392.

Sirak, Adjmal S. 2015. "Income and Unemployment Effects on Life Insurance Lapse." .

Society of Actuaries. 2010. "Report on the Lapse and Mortality Experience of Post-Level Premium Period Term Plans."

Society of Actuaries and LIMRA. 2012. "U.S. Individual Life Insurance Persistency: A Joint Study Sponsored by the Society of Actuaries and LIMRA."

———. 2019. "U.S. Individual Life Insurance Persistency: A Joint Study Sponsored by the Society of Actuaries and LIMRA."

Stanton, Richard. 1995. "Rational Prepayment and the Valuation of Mortgage-Backed Securities." *Review of Financial Studies* 8 (3):677–708.

Zhang, David. 2022. "Closing Costs, Refinancing, and Inefficiencies in the Mortgage Market." Working Paper.

A Model Solution

A.1 Nominal Bonds

Proposition 1. Nominal bond yields are affine in the state vector:

$$y_t^{\$}(\tau) = -\frac{A_\tau^{\$}}{\tau} - \frac{B_\tau^{\$\prime}}{\tau} z_t,$$

where the coefficients $A_\tau^{\$}$ and $B_\tau^{\$}$ satisfy the following recursions:

$$A_{\tau+1}^{\$} = A_\tau^{\$} + \frac{1}{2}\left(B_\tau^{\$}\right)' \Sigma \left(B_\tau^{\$}\right) + \left(B_\tau^{\$}\right)' \left(\mu - \Sigma^{\frac{1}{2}} \Lambda_0\right), \tag{A.1}$$

$$\left(B_{\tau+1}^{\$}\right)' = \left(B_\tau^{\$}\right)' \left(\Psi - \Sigma^{\frac{1}{2}} \Lambda_1\right) - e_{yn}', \tag{A.2}$$

initialized at $A_0^{\$} = 0$ and $B_0^{\$} = 0$.

Proof. We conjecture that the $t+1$-price of a τ-period bond is exponentially affine in the state:

$$\log(P_{t+1,\tau}^{\$}) = A_\tau^{\$} + \left(B_\tau^{\$}\right)' z_{t+1}$$

and solve for the coefficients $A_{\tau+1}^{\$}$ and $B_{\tau+1}^{\$}$ in the process of verifying this conjecture using the Euler equation:

$$\begin{aligned} P_{t,\tau+1}^{\$} &= \mathbb{E}_t[\exp\{m_{t+1}^{\$} + \log\left(P_{t+1,\tau}^{\$}\right)\}] \\ &= \mathbb{E}_t[\exp\{-y_{t,1}^{\$} - \frac{1}{2}\Lambda_t'\Lambda_t - \Lambda_t'\varepsilon_{t+1} + A_\tau^{\$} + \left(B_\tau^{\$}\right)' z_{t+1}\}] \\ &= \exp\{-e_{yn}' z_t - \frac{1}{2}\Lambda_t'\Lambda_t + A_\tau^{\$} + \left(B_\tau^{\$}\right)'(\mu + \Psi z_t)\} \times \\ &\quad \mathbb{E}_t\left[\exp\{-\Lambda_t'\varepsilon_{t+1} + \left(B_\tau^{\$}\right)' \Sigma^{\frac{1}{2}} \varepsilon_{t+1}\}\right]. \end{aligned}$$

We use the log-normality of ε_{t+1} and substitute for the affine expression for Λ_t to get:

$$P_{t,\tau+1}^{\$} = \exp\left\{-e_{yn}' z_t + A_\tau^{\$} + \left(B_\tau^{\$}\right)'(\mu + \Psi z_t) + \frac{1}{2}\left(B_\tau^{\$}\right)' \Sigma \left(B_\tau^{\$}\right) - \left(B_\tau^{\$}\right)' \Sigma^{\frac{1}{2}} (\Lambda_0 + \Lambda_1 z_t)\right\}.$$

Taking logs and collecting terms, we obtain a linear equation for $\log(p_t(\tau+1))$:

$$\log\left(P_{t,\tau+1}^{\$}\right) = A_{\tau+1}^{\$} + \left(B_{\tau+1}^{\$}\right)' z_t,$$

where $A_{\tau+1}^{\$}$ satisfies (A.1) and $B_{\tau+1}^{\$}$ satisfies (A.2). The relationship between log bond prices

and bond yields is given by $-\log\left(P^{\$}_{t,\tau}\right)/\tau = y^{\$}_{t,\tau}$. □

A.2 Term Life Policy

The solution depends on the lapse factor exposures at different policy age, i.e. $b^{(1:\tau)} = \left\{b^{(1)}, b^{(2)}, \cdots, b^{(\tau)}\right\}$. We recursively solve for the two coefficient functions $P_\tau : \mathbb{R}^\tau \to \mathbb{R}$ and $Q_\tau : \mathbb{R}^\tau \to \mathbb{R}^N$ that satisfy $\mathbb{E}_t\left[M^{\$}_{t,1:\tau}\prod_{s=1}^{\tau}(1-\lambda^{(s)}_{t+s})\right] = \exp\left(P_\tau(b^{(1:\tau)}) + Q_\tau(b^{(1:\tau)})' z_t\right)$. The other term $\mathbb{E}_t\left[M^{\$}_{t,1:\tau}\prod_{s=1}^{\tau-1}(1-\lambda^{(s)}_{t+s})\right]$ in the numerator can be calculated as a special case when $b^{(\tau)} = 0$, that is, if there is no lapsation in the final period. The following proposition provides the recursion for P_τ and Q_τ. Note that when $\tau = 0$, we slightly abuse the notation $P_\tau(b^{(2:\tau+1)}) = P_0$ and $Q_\tau(b^{(2:\tau+1)}) = Q_0$ for constants P_0 and Q_0 for simplicity.

Proposition 2. Term policy price p can be written as:

$$p = (1+\phi)\frac{\sum_{\tau=1}^{T}\exp\left(P_\tau(b^{(1:\tau-1)},0) + Q_\tau(b^{(1:\tau-1)},0)' z_t\right)\pi_{a+\tau-1}\prod_{s=1}^{\tau-1}(1-\pi_{a+s-1})}{1+\sum_{\tau=1}^{T-1}\exp\left(P_\tau(b^{(1:\tau)}) + Q_\tau(b^{(1:\tau)})' z_t\right)\prod_{s=1}^{\tau}(1-\pi_{a+s-1}) - \kappa},$$

where the coefficient functions $P_\tau : \mathbb{R}^\tau \to \mathbb{R}$ and $Q_\tau : \mathbb{R}^\tau \to \mathbb{R}^N$ satisfy the following recursions:

$$\begin{aligned} P_{\tau+1}(b^{(1:\tau+1)}) &= -b^{(1)}a_0 + P_\tau(b^{(2:\tau+1)}) + \left(Q_\tau(b^{(2:\tau+1)}) - b^{(1)}a_1\right)'\left(\mu - \Sigma^{\frac{1}{2}}\Lambda_0\right) \\ &\quad + \frac{1}{2}\left(Q_\tau(b^{(2:\tau+1)}) - b^{(1)}a_1\right)'\Sigma\left(Q_\tau(b^{(2:\tau+1)}) - b^{(1)}a_1\right), \qquad \text{(A.3)} \\ \left(Q_{\tau+1}(b^{(1:\tau+1)})\right)' &= \left(Q_\tau(b^{(2:\tau+1)}) - b^{(1)}a_1\right)'\left(\Psi - \Sigma^{\frac{1}{2}}\Lambda_1\right) - e'_{yn}, \qquad \text{(A.4)} \end{aligned}$$

initialized at $P_0 = 0$ and $Q_0 = 0$.

Proof. We conjecture the exponential affine form solution,

$$\mathbb{E}_t\left[M^{\$}_{t,1:\tau}\prod_{s=1}^{\tau}(1-\lambda^{(s)}_{t+s})\right] = \exp\left(P_\tau(b^{(1:\tau)}) + Q_\tau(b^{(1:\tau)})' z_t\right).$$

Then we can recursively calculate $\mathbb{E}_t\left[M^{\$}_{t,1:\tau+1}\prod_{s=1}^{\tau+1}(1-\lambda^{(s)}_{t+s})\right]$ as follows, using the concise notation $\vec{b} = b^{(2:\tau+1)}$,

$$
\begin{aligned}
&\mathbb{E}_t\left[\prod_{s=1}^{\tau+1}\exp(m^{\$}_{t+s}-b^{(s)}\tilde{l}_{t+s})\right]\\
&=\mathbb{E}_t\left[\exp(m^{\$}_{t+1}-b^{(1)}\tilde{l}_{t+1})\mathbb{E}_{t+1}\left[\prod_{s=1}^{\tau}\exp(m^{\$}_{t+1+s}-b^{(s+1)}\tilde{l}_{t+1+s})\right]\right]\\
&=\mathbb{E}_t\left[\exp(m^{\$}_{t+1}-b^{(1)}\tilde{l}_{t+1})\exp\left[P_\tau(b^{(2:\tau+1)})+Q_\tau(b^{(2:\tau+1)})'z_{t+1}\right]\right]\\
&=\mathbb{E}_t\exp\left[(-e'_{yn}z_t-\frac{1}{2}\Lambda_t'\Lambda_t-\Lambda_t'\epsilon_{t+1}-b^{(1)}(a_0+a_1'z_{t+1})+P_\tau(\vec{b})+Q_\tau(\vec{b})'z_{t+1})\right]\\
&=\mathbb{E}_t\exp\left[(-e'_{yn}z_t-\frac{1}{2}\Lambda_t'\Lambda_t-\Lambda_t'\epsilon_{t+1}-b^{(1)}a_0+P_\tau(\vec{b}))+(Q_\tau(\vec{b})-b^{(1)}a_1)'z_{t+1})\right]\\
&=\mathbb{E}_t\exp\Bigg[(-e'_{yn}z_t-\frac{1}{2}\Lambda_t'\Lambda_t-\Lambda_t'\epsilon_{t+1}-b^{(1)}a_0+P_\tau(\vec{b}))\\
&\qquad+(Q_\tau(\vec{b})-b^{(1)}a_1)'(\mu+\Psi z_t+\Sigma^{\frac{1}{2}}\varepsilon_{t+1}))\Bigg]\\
&=\mathbb{E}_t\exp\Bigg[(-\frac{1}{2}\Lambda_t'\Lambda_t-b^{(1)}a_0+P_\tau(\vec{b}))+(Q_\tau(\vec{b})-b^{(1)}a_1)'\mu\\
&\qquad+((Q_\tau(\vec{b})-b^{(1)}a_1)'\Psi-e'_{yn})z_t+((Q_\tau(\vec{b})-b^{(1)}a_1)'\Sigma^{\frac{1}{2}}-\Lambda_t')\varepsilon_{t+1}\Bigg]\\
&=\exp\Bigg[-b^{(1)}a_0+P_\tau(\vec{b})+(Q_\tau(\vec{b})-b^{(1)}a_1)'\mu+((Q_\tau(\vec{b})-b^{(1)}a_1)'\Psi-e'_{yn})z_t\\
&\qquad+\frac{1}{2}(Q_\tau(\vec{b})-b^{(1)}a_1)'\Sigma(Q_\tau(\vec{b})-b^{(1)}a_1)-(Q_\tau(\vec{b})-b^{(1)}a_1)'\Sigma^{\frac{1}{2}}(\Lambda_0+\Lambda_1 z_t)\Bigg]\\
&=\exp\Bigg[-b^{(1)}a_0+P_\tau(\vec{b})+(Q_\tau(\vec{b})-b^{(1)}a_1)'(\mu-\Sigma^{\frac{1}{2}}\Lambda_0)\\
&\qquad+\frac{1}{2}(Q_\tau(\vec{b})-b^{(1)}a_1)'\Sigma(Q_\tau(\vec{b})-b^{(1)}a_1)\\
&\qquad+((Q_\tau(\vec{b})-b^{(1)}a_1)'(\Psi-\Sigma^{\frac{1}{2}}\Lambda_1)-e'_{yn})z_t\Bigg].
\end{aligned}
$$

Taking the logs and collecting terms, we obtain a linear equation:

$$
\log\left(\mathbb{E}_t\left[M^{\$}_{t,1:\tau+1}\prod_{s=1}^{\tau+1}(1-\lambda^{(s)}_{t+s})\right]\right)=P_{\tau+1}(b^{(1:\tau+1)})+Q_{\tau+1}(b^{(1:\tau+1)})'z_t,
$$

where the coefficient functions satisfy

$$P_{\tau+1}(b^{(1:\tau+1)}) = -b^{(1)}a_0 + P_\tau(b^{(2:\tau+1)}) + (Q_\tau(b^{(2:\tau+1)}) - b^{(1)}a_1)'(\mu - \Sigma^{\frac{1}{2}}\Lambda_0) + \frac{1}{2}(Q_\tau(b^{(2:k+1)}) - b^{(1)}a_1)'\Sigma(Q_\tau(b^{(2:\tau+1)}) - b^{(1)}a_1), \tag{A.5}$$

and

$$Q_{\tau+1}(b^{(1:\tau+1)})' = (Q_\tau(b^{(2:\tau+1)}) - b^{(1)}a_1)'(\Psi - \Sigma^{\frac{1}{2}}\Lambda_1) - e'_{yn}. \tag{A.6}$$

Substituting $\mathbb{E}_t\left[M^{\$}_{t,1:\tau}\prod_{s=1}^{\tau}(1-\lambda^{(s)}_{t+s})\right] = \exp\left(P_\tau(b^{(1:\tau)}) + Q_\tau(b^{(1:\tau)})z_t\right)$ into Equation (8) concludes the proof.

Note that if we evaluate the coefficients with $b^{(n)} = 0, \forall n$, then $\{P_\tau, Q_\tau\}$ do not depend on b anymore, so we get the following recursion for the affine coefficient constants $\{ZP_\tau, ZQ_\tau\}$ for the zero coupon bonds Z_τ (i.e. $Z_\tau = \mathbb{E}_t\left[M^{\$}_{t,t+1:t+\tau}\right] = \exp\left[ZP_\tau + ZQ_\tau{}'z_t\right]$)

$$\begin{aligned} ZP_{\tau+1} &= ZP_\tau + ZQ_\tau{}'(\mu - \Sigma^{\frac{1}{2}}\Lambda_0) + \frac{1}{2}ZQ_\tau{}'\Sigma ZQ_\tau, \\ ZQ_{\tau+1}{}' &= ZQ_\tau{}'(\Psi - \Sigma^{\frac{1}{2}}\Lambda_1) - e'_{yn}. \end{aligned}$$

We can analogously calculate the coefficient function recursion for the expected survival function, $L_\tau(b^{(1:\tau)}) = \mathbb{E}_t\left[\prod_{s=1}^{\tau}(1-\lambda^{(s)}_{t+s})\right] = \exp\left[LP_\tau(b^{(1:\tau)}) + LQ_\tau(b^{(1:\tau)})'z_t\right]$

$$\begin{aligned} LP_{\tau+1}(b^{(1:\tau+1)}) &= -b^{(1)}a_0 + LP_\tau(b^{(2:\tau+1)}) + (LQ_\tau(b^{(2:\tau+1)}) - b^{(1)}a_1)'\mu \\ &\quad + \frac{1}{2}(LQ_\tau(b^{(2:\tau+1)}) - b^{(1)}a_1)'\Sigma(LQ_\tau(b^{(2:\tau+1)}) - b^{(1)}a_1), \\ LQ_{\tau+1}(b^{(1:\tau+1)})' &= (LQ_\tau(b^{(2:\tau+1)}) - b^{(1)}a_1)'\Psi. \end{aligned}$$

□

The recursion in Proposition 2 can be regarded as an extension of the recursion in Proposition 1. When lapse rates do not depend on the state of the economy, i.e. $b^{(1)} = b^{(2)} = \cdots = b^{(\tau)} = 0$, $\mathbb{E}_t\left[M^{\$}_{t,1:\tau}\prod_{s=1}^{\tau}(1-\lambda^{(s)}_{t+s})\right]$ simplifies to the nominal bond price of maturity τ. We verify that $P_\tau(\vec{0}) = A^{\$}_\tau$ and $Q_\tau(\vec{0}) = B^{\$}_\tau$. Indeed, Equations (A.5) and (A.6) are equivalent to Equations (6) and (7) when $b^{(1)} = b^{(2)} = \cdots = b^{(\tau+1)} = 0$.

B Monthly VAR Model Calibration with Annual Data

B.1 Model Setup

We follow the set up described in Section 5.5. The monthly state variables $z_t = (r_t, cr_t, s_t)'$ follows the dynamics

$$z_t = \mu + \Psi z_{t-1} + \Sigma^{\frac{1}{2}} \varepsilon_t \tag{B.1}$$

The monthly dynamics implies the following two annual dynamics

$$z_{t+k} = \left(\sum_{i=0}^{k-1} \Psi^i \right) \mu + \Psi^k z_t + \sum_{i=0}^{k-1} \Psi^i \Sigma^{\frac{1}{2}} \varepsilon_{t+k-i}, \tag{B.2}$$

and

$$\sum_{k=1}^{K} z_{t+k} = \sum_{k=1}^{K} \left(\sum_{i=0}^{k-1} \Psi^i \right) \mu + \sum_{k=1}^{K} \Psi^k z_t + \sum_{k=1}^{K} \sum_{i=0}^{k-1} \Psi^i \Sigma^{\frac{1}{2}} \varepsilon_{t+k-i}. \tag{B.3}$$

Equation (B.2) describes the dynamics of the annually observed interest rate and the credit spread (r_{t+12} and s_{t+12}), while Equation (B.3) describes the annually observed credit return ($\sum_{k=1}^{12} cr_{t+k}$).

The monthly nominal SDF $M^{\$}_{t+1} = \exp(m^{\$}_{t+1})$ becomes

$$m^{\$}_{t+1} = -\frac{\delta_0}{12} - \frac{\delta_1' z_t}{12} - \frac{1}{2} \Lambda_t' \Lambda_t - \Lambda_t' \varepsilon_{t+1}. \tag{B.4}$$

where the one-month discount rate $y^{\$}_{t,1} = \dfrac{\delta_0}{12} + \dfrac{\delta_1' z_t}{12}$ is an affine form of the state variable z_t. We parameterize the market price of risk Λ_t as

$$\Lambda_t = \Lambda_0 + \Lambda_1 z_t = \Lambda_0 + \hat{\Lambda}_1 e_3' z_t$$

which requires us to identify three parameters, two for $\Lambda_0 = (\Lambda_0^r, \Lambda_0^{cr}, 0)'$ and one for $\hat{\Lambda}_1 = (0, \zeta, 0)'$.

We additionally model the credit return as

$$cr_{t+1} - y^{\$}_{t,1} = \gamma_0 + \gamma_1 s_t + \sigma^{cr} e_{t+1} \tag{B.5}$$

with $e_{t+1} \sim \mathcal{N}(0,1)$, so that the expected excess return depends on the credit spread.

Note that the recursions in Proposition 1 and Proposition 2 in Appendix A are slightly

changed in the monthly model, as the discount rate is now an affine form of the states, not simply the first state. More precisely, Equation (A.1) and (A.2) become

$$A^{\$}_{\tau+1} = -\frac{\delta_0}{12} + A^{\$}_{\tau} + \frac{1}{2}\left(B^{\$}_{\tau}\right)' \Sigma \left(B^{\$}_{\tau}\right) + \left(B^{\$}_{\tau}\right)' \left(\mu - \Sigma^{\frac{1}{2}}\Lambda_0\right), \tag{B.6}$$

$$\left(B^{\$}_{\tau+1}\right)' = \left(B^{\$}_{\tau}\right)' \left(\Psi - \Sigma^{\frac{1}{2}}\Lambda_1\right) - \frac{\delta_1'}{12} \tag{B.7}$$

and Equations (A.3) and (A.4) become

$$\begin{aligned} P_{\tau+1}(b^{(1:\tau+1)}) = & -\frac{\delta_0}{12} - b^{(1)}a_0 + P_{\tau}(b^{(2:\tau+1)}) + \left(Q_{\tau}(b^{(2:\tau+1)}) - b^{(1)}a_1\right)' \left(\mu - \Sigma^{\frac{1}{2}}\Lambda_0\right) \\ & + \frac{1}{2}\left(Q_{\tau}(b^{(2:\tau+1)}) - b^{(1)}a_1\right)' \Sigma \left(Q_{\tau}(b^{(2:\tau+1)}) - b^{(1)}a_1\right) \end{aligned} \tag{B.8}$$

$$\left(Q_{\tau+1}(b^{(1:\tau+1)})\right)' = \left(Q_{\tau}(b^{(2:\tau+1)}) - b^{(1)}a_1\right)' \left(\Psi - \Sigma^{\frac{1}{2}}\Lambda_1\right) - \frac{\delta_1'}{12}. \tag{B.9}$$

B.2 Calibration Process

Note that given our specification of Λ_0 and Λ_1, all the affine coefficients for the yields $\{B^{\$}_{\tau}\}_{\forall\tau}$ have the second and the third components zeros (see Equation B.7), so we can simplify to $\delta_1 = (\hat{\delta}_1, 0, 0)$ and only need to estimate $\hat{\delta}_1$. Then the short rate then becomes $12y^{\$}_{t,1} = \delta_0 + \delta_1' z_t = \delta_0 + \hat{\delta}_1 r_t$.

We start by restricting the companion matrix as

$$\Psi = \begin{bmatrix} \phi_r & 0 & 0 \\ \frac{\hat{\delta}_1}{12} & 0 & \gamma_1 \\ 0 & 0 & \phi_s \end{bmatrix}$$

The restriction in the second row directly follows from our credit return model in Equation (B.5). For r_t and s_t, we set the off-diagonal terms zero. For the covariance matrix, we specify is as a lower triangular matrix

$$\Sigma^{\frac{1}{2}} = \begin{bmatrix} \sigma^{11} & 0 & 0 \\ \sigma^{21} & \sigma^{22} & 0 \\ \sigma^{31} & \sigma^{32} & \sigma^{33} \end{bmatrix}$$

The monthly persistence parameters (ϕ_r, ϕ_s) are estimated by regressing r_{t+12} on r_t and s_{t+12}

on s_t, as Equation (B.2) implies

$$r_{t+12} = e_1' \left(\sum_{i=0}^{k-1} \Psi^i \right) \mu + e_1' \Psi^k z_t + e_1' \sum_{i=0}^{11} \Psi^i \Sigma^{\frac{1}{2}} \varepsilon_{t+12-i} \tag{B.10}$$

$$s_{t+12} = e_3' \left(\sum_{i=0}^{k-1} \Psi^i \right) \mu + e_3' \Psi^k z_t + e_3' \sum_{i=0}^{11} \Psi^i \Sigma^{\frac{1}{2}} \varepsilon_{t+12-i}. \tag{B.11}$$

That is, Ψ^{12} is the annual companion matrix. The estimated annual persistence implies $\phi_r^{12} = 0.7770$ and $\phi_s^{12} = 0.2431$, so we get $\phi_r = 0.9792$ and $\phi_s = 0.8888$. We estimate $\mu^r = 0.0006$ and $\mu^s = 0.0026$ to match the unconditional r_t, s_t implied by Equation (B.2) with the 1990-2020 mean in the data, 0.0276 and 0.0237.

Equation (B.10) also implies that the error term of r_{t+12} on r_t regression is $e_1' \sum_{i=0}^{11} \Psi^i \Sigma^{\frac{1}{2}} \varepsilon_{t+12-i}$. Then the variance of the error term becomes

$$Var_t[e_1' \sum_{i=0}^{11} \Psi^i \Sigma^{\frac{1}{2}} \varepsilon_{t+12-i}] = \sum_{i=0}^{11} e_1' \Psi^i \Sigma (\Psi^i)' e_1 \tag{B.12}$$

which implies $\sigma^{11} = 0.0041$.

We then estimate $(\Lambda_0^r, \delta_0, \hat{\delta}_1)$ using the following three moment conditions. First, we match the unconditional slope of the yield curve between the 1-year and 10-year log rates, which is 0.136 in the 1990-2020 annual data. We also match $A_{12}^{\$} = 0$ and $B_{12}^{\$} = (-1, 0, 0)$ conditions. Note that given our risk price assumption, knowing μ^r and σ^{11} is sufficient to generate the entire yield curve. The estimated parameters are $\Lambda_0^r = -0.1265$, $\delta_0 = -0.0062$ and $\hat{\delta}_1 = 1.1196$.

Now we estimate γ_1. First, observe that the dynamics of $\sum_{k=1}^{12} cr_{t+k}$ is implied by Equation (B.3)

$$\sum_{k=1}^{12} cr_{t+k} = e_2' \sum_{k=1}^{12} \left(\sum_{i=0}^{k-1} \Psi^i \right) \mu + e_2' \sum_{k=1}^{12} \Psi^k z_t + e_2' \sum_{k=1}^{12} \sum_{i=0}^{k-1} \Psi^i \Sigma^{\frac{1}{2}} \varepsilon_{t+k-i} \tag{B.13}$$

Observe that $e_2' \sum_{k=1}^{12} \Psi^k = (1, 0, \left(\sum_{i=0}^{11} \phi_s^i \right) \gamma_1)$. Therefore if we regress $\left(\sum_{k=1}^{12} cr_{t+k} \right) - r_t$ on s_t, i.e. if we run the annual credit excess return predictive regression, the estimated annual prediction coefficient 4.9324 implies $\gamma_1 = 0.7245$. By matching the unconditional credit excess return, we get $\mu^{cr} = -0.0139$.

The rest five elements of $\Sigma^{\frac{1}{2}}$ can be estimated from Equation (B.10), (B.11), and (B.13), which imply 5 covariance equations in addition to Equation (B.12) we already used. For example, the model implied covariance between the residuals of r_{t+12} equation and $\sum_{k=1}^{12} cr_{t+k}$

equation is:

$$Cov_t[e_1' \sum_{i=0}^{11} \Psi^i \Sigma^{\frac{1}{2}} \varepsilon_{t+12-i}, e_2' \sum_{k=1}^{12} \sum_{i=0}^{k-1} \Psi^i \Sigma^{\frac{1}{2}} \varepsilon_{t+k-i}]$$

which should match the (1, 2)-th element of the residual covariance matrix from the regressions in Equation (B.10), (B.11), and (B.13) using the annual data. The estimated $\Sigma^{\frac{1}{2}}$ is:

$$\Sigma^{\frac{1}{2}} = \begin{bmatrix} 0.0041 & 0 & 0 \\ 0.0013 & 0.0242 & 0 \\ -0.0023 & -0.0025 & 0.0016 \end{bmatrix}$$

We conclude the calibration process by estimating the rest two market price of risks, Λ_0^{cr} and ζ. We use the conditions from the credit return Euler equations, Equation (13) and (14) that we specify in Section 5.5 as moment conditions:

$$\gamma_0 + \gamma_1 E[s_t] + \frac{1}{2}(\sigma^{cr})^2 = \Lambda_0^r \sigma^{cr} Cov[e_{t+1}, \varepsilon_{t+1}^r] + (\Lambda_0^{cr} + \zeta E[s_t]) \sigma^{cr} Cov[e_{t+1}, \varepsilon_{t+1}^{cr}] \tag{B.14}$$

$$\gamma_1 = \zeta \sigma^{cr} Cov[e_{t+1}, \varepsilon_{t+1}^{cr}] \tag{B.15}$$

where $(\sigma^{cr})^2 = \Sigma_{2,2}$, $\sigma^{cr} Cov[e_{t+1}, \varepsilon_{t+1}^r] = \Sigma_{2,1}^{\frac{1}{2}}$, and $\sigma^{cr} Cov[e_{t+1}, \varepsilon_{t+1}^{cr}] = \Sigma_{2,2}^{\frac{1}{2}}$. The estimated parameters are $\Lambda_0^{cr} = -0.5365$ and $\zeta = 29.98$.

B.3 Mispricing Calculation with Monthly VAR Model

Proposition 2 assumes the annual VAR model. Pricing formula and mispricing calculation should be slightly modified to reflect the fact that (i) we model the underlying monthly VAR model, and (ii) we model the lapse factor as a function of the 12-month moving average of the states, i.e. $\tilde{l}_t = a_0 + a_1' \bar{z}_t$. Equation (B.6), (B.7), (B.8), and (B.9) show how the recursions change due to the monthly SDF specification (effect of (i)). We additionally modify the recursions Equation (B.8) and (B.9) in this section (effect of (ii)).

We extend the state space to include the 11 lagged state variables, i.e. $y_t' = (z_t', z_{t-1}', \cdots, z_{t-11}')$. Then the dynamics of y_t is derived from Equation (B.1):

$$y_t = \tilde{\mu} + \tilde{\Psi} y_{t-1} + \tilde{\Sigma}^{\frac{1}{2}} \varepsilon_t$$

where the new parameters $(\tilde{\mu}, \tilde{\Psi}, \tilde{\Sigma}^{\frac{1}{2}})$ can be naturally extended from $(\mu, \Psi, \Sigma^{\frac{1}{2}})$ by padding zeros and identity matrices. We can similarly extend the time-varying component of MPR Λ_1 to $\tilde{\Lambda}_1$. We omit the details for brevity.

We can also transform the parameters $a_0, a_1, \{b^{(n)}\}$ to be consistent with the extended state space. The lapse factor can be written as $\tilde{l}_t = a_0 + a_1'\bar{z}_t = a_0 + \tilde{a}_1' y_t$, where $\tilde{a}_1' = (\frac{1}{12}, \frac{1}{12}, \ldots, \frac{1}{12}) \otimes a_1'$. Also define $\{\tilde{b}^{(n)}\}_{1 \le n \le 240}$ as

$$\tilde{b}^{(n)} = \begin{cases} 0 & if \mod (n, 12) \neq 0 \\ b^{(n/12)} & if \mod (n, 12) = 0 \end{cases}$$

Then we can calculate the monthly recursions similar to Proposition 2,

$$\begin{aligned} P_{\tau+1}(\tilde{b}^{(1:\tau+1)}) &= -\frac{\delta_0}{12} - \tilde{b}^{(1)} a_0 + P_\tau(\tilde{b}^{(2:\tau+1)}) + \left(Q_\tau(\tilde{b}^{(2:\tau+1)}) - \tilde{b}^{(1)}\tilde{a}_1\right)' \left(\tilde{\mu} - \tilde{\Sigma}^{\frac{1}{2}}\Lambda_0\right) \\ &\quad + \frac{1}{2}\left(Q_\tau(\tilde{b}^{(2:\tau+1)}) - \tilde{b}^{(1)}\tilde{a}_1\right)' \tilde{\Sigma} \left(Q_\tau(\tilde{b}^{(2:\tau+1)}) - \tilde{b}^{(1)}\tilde{a}_1\right) \qquad \text{(B.16)} \\ \left(Q_{\tau+1}(\tilde{b}^{(1:\tau+1)})\right)' &= \left(Q_\tau(\tilde{b}^{(2:\tau+1)}) - \tilde{b}^{(1)}\tilde{a}_1\right)' \left(\tilde{\Psi} - \tilde{\Sigma}^{\frac{1}{2}}\tilde{\Lambda}_1\right) - \frac{\delta_1'}{12}. \qquad \text{(B.17)} \end{aligned}$$

Note that after calculating the monthly coefficient recursions, we still calculate the premium leg and the death benefit leg value by summing up annual strips, where the τth-year strip is calculated by:

$$E_t\left[M^{\$}_{t,1:\tau} \prod_{s=1}^{\tau} (1 - \lambda^{(s)}_{t+s})\right] = \exp\left(P_{12*\tau}(\tilde{b}^{(1:12*\tau)}) + Q_{12*\tau}(\tilde{b}^{(1:12*\tau)})' y_t\right).$$

C Markup Validation with Expected Profit Share

The life insurer sets ϕ as the markup on the policy before considering the brokerage fee. From the net premium (the expected premium income net of the expected benefit payout) the insurer first pays the broker fee and the rest is the earned profit. In presenting mispricing results, we vary ϕ to take values of 5%, 10%, and 20%. To validate whether these values are realistic, we calculate the expected profit split of $\theta : (1-\theta)$ between the insurer and the broker, where $0 < \theta < 1$ indicates the life insurer's profit share and the $(1-\theta)$ indicates the broker's fee share. The premium pricing formula from Section 5.6 is

$$\begin{aligned}\tilde{p} &= (1+\phi)\frac{\sum_{\tau=1}^{T}\mathbb{E}_t\left[M^{\$}_{t,1:\tau}\prod_{s=1}^{\tau-1}(1-\lambda^{(s)}_{t+s})\right]\mathbb{E}_t\left[\pi_{a+\tau-1}\prod_{s=1}^{\tau-1}(1-\pi_{a+s-1})\right]}{1+\sum_{\tau=1}^{T-1}\mathbb{E}_t\left[M^{\$}_{t,1:\tau}\prod_{s=1}^{\tau}(1-\lambda^{(s)}_{t+s})\right]\mathbb{E}_t\left[\prod_{s=1}^{\tau}(1-\pi_{a+s-1})\right]-\kappa}, \\ &= (1+\phi)\frac{\tilde{\beta}(T)}{\tilde{\alpha}(T)-\kappa}\end{aligned}$$

The second line follows from our assumption that the life insurer is pricing premium with markup ϕ without the aggregate lapsation risk. Thus, the expectation operator in the denominator is evaluated to be $\tilde{\alpha}(T)$ instead of $\alpha(T)$, using the notation from Section 5.6.

The life insurer expects $\phi\tilde{\beta}(T)$ as its profit, while the broker receives the fee $\kappa \cdot \tilde{p}$. Therefore, the expected profit share of the insurer is

$$\begin{aligned}\theta &= \frac{\phi\tilde{\beta}(T)}{\phi\tilde{\beta}(T)+\kappa\cdot\tilde{p}} \\ &= \frac{\tilde{\alpha}(T)-\kappa}{(1+\phi^{-1})+\tilde{\alpha}(T)-\kappa}\end{aligned}$$

The formula is consistent with our intuition as the expected profit share θ is higher when the markup (ϕ) is higher and the the broker fee (κ) is lower.

Table A1 shows the expected profit share θ calculated for the ranges of parameters for ϕ and κ we consider in Table 8. In our baseline case of $\phi = 10\%$ and $\kappa = 0.75$, the expected profit share is between 40% to 50%, which is within the range of the industry consensus.

D Additional Tables and Figures

Table A1. **Expected Profit Share**

This table presents the expected profit share θ calculated for the ranges of parameters for ϕ and κ we consider in Table 8. See Appendix C for the details.

		κ=0.5	κ=0.75	κ=1.0
10-year Term Policy	ϕ= 5%	36.0%	26.4%	20.5%
	ϕ= 10%	51.8%	40.6%	32.9%
	ϕ= 20%	66.3%	55.7%	47.4%
15-year Term Policy	ϕ= 5%	41.3%	31.1%	24.7%
	ϕ= 10%	57.3%	46.3%	38.5%
	ϕ= 20%	71.1%	61.3%	53.4%
20-year Term Policy	ϕ= 5%	44.1%	33.8%	27.0%
	ϕ= 10%	60.1%	49.3%	41.4%
	ϕ= 20%	73.4%	64.1%	56.5%

Table A2. **Lapse Rate Change against County-level Economic Variables: OLS**

This table reports the county-level regression of the change in lapse rates between 2006 and 2009 on the changes in economic variables between 2006 and 2009. We estimate the following cross-sectional regression:

$$(\Delta Lapse06-09)_c = \beta_0 + \beta_1 * (\Delta HousingPrice06-09)_c + \beta_2 * (\Delta Unemp06-09)_c + \gamma * X_c + \varepsilon_c.$$

Robust standard errors are reported.

	Lapse Chg (1)	Lapse Chg (2)	Lapse Chg (3)	Lapse Chg (4)	Lapse Chg (5)	Lapse Chg (6)	Lapse Chg (7)	Lapse Chg (8)	Lapse Chg (9)
Δ Housing Price 06-09	-0.03956***	-0.03710**	-0.03595**				-0.02534	-0.01619	-0.01441
	(0.01370)	(0.01467)	(0.01476)				(0.01618)	(0.01846)	(0.01879)
Δ Unemp 06-09				0.31207***	0.32883***	0.32494***	0.20614	0.25729*	0.26104*
				(0.10234)	(0.10292)	(0.10290)	(0.12606)	(0.13471)	(0.13568)
ACS Income 2006		0.00009	0.00008		0.00024*	0.00021		0.00020	0.00019
		(0.00014)	(0.00014)		(0.00013)	(0.00013)		(0.00015)	(0.00015)
Log Population 2006			0.00015			0.00033			0.00019
			(0.00044)			(0.00040)			(0.00044)
Constant	0.00590***	0.00174	0.00063	-0.00531	-0.01780**	-0.01969**	-0.00208	-0.01360	-0.01523
	(0.00214)	(0.00741)	(0.00818)	(0.00464)	(0.00873)	(0.00912)	(0.00495)	(0.01059)	(0.01145)
R^2	0.01037	0.01075	0.01096	0.01148	0.01483	0.01589	0.01402	0.01583	0.01616
Adj R^2	0.00906	0.00815	0.00705	0.01028	0.01243	0.01228	0.01141	0.01192	0.01094
N	762	762	762	823	823	823	759	759	759

Standard errors in parentheses

* p<0.1, ** p<0.05, *** p<0.01

Table A3. **Estimated Cluster Centers using ZIP-code level Characteristics**

This table presents the estimated cluster centers from the K-nearest neighbor (KNN) algorithm described in Section 4. The ZIP-code level characteristics (log of average income, *Minority*, *College+*, *HomeOwnership*) are standardized before running the standard KNN algorithm with K = 3. In the second column, we report the exponentiated value of the log income. The estimated clusters are labeled based on the observed characteristics. Cluster 3 represents the high-income group, while Cluster 1 and 2 represent the low-income groups. Cluster 1 and 2 are mainly distinguished by the marked difference in the fraction of minority.

Cluster Mean	Avg Income (000s)	College+ (%)	Minority (%)	HomeOwnership %	Sample Distribution
Cluster 1: Mid-income, High Minority	50	27.4	54.3	49.1	21.5%
Cluster 2: High Income	155	63.3	13.1	69.6	30.4%
Cluster 3: Mid-income, Low Minority (omitted)	68	32.9	14.5	73.1	48.1%

Table A4. **Proportional Hazard Model Estimation with ZIP-code level Characteristics**

This table presents the Cox proportional hazard model estimation results with the ZIP-code level characteristics (income, race, education, homeownership) instead of the cluster information in Table 6. The ZIP-code level income data is from IRS SOI and the race, education, and homeownership data is from Census. See Section 4 for the details of the variable construction.

ZipCode-level Characteristic Included	**Income Only**		**Race Only**		**Education Only**		**Housing Only**		**All**	
	β	t-stat	β	t-stat	β	t-stat	β	t-stat	β	t-stat
Age Group 00-29	0.40	43.16	0.42	45.11	0.41	44.13	0.42	45.56	0.40	43.14
Age Group 30-39	0.12	23.10	0.13	24.50	0.13	23.80	0.13	24.86	0.12	23.18
Age Group 50-59	0.09	15.56	0.09	16.72	0.09	15.55	0.09	16.29	0.09	15.76
Age Group 60 or higher	0.02	2.71	0.03	4.75	0.02	2.84	0.03	3.71	0.02	3.23
Age Group 00-29 x LapseCycle	-0.02	-1.46	-0.02	-1.48	-0.02	-1.41	-0.02	-1.42	-0.02	-1.66
Age Group 30-39 x LapseCycle	-0.01	-1.71	-0.02	-1.85	-0.02	-1.78	-0.02	-1.86	-0.01	-1.66
Age Group 50-59 x LapseCycle	-0.15	-16.19	-0.15	-15.84	-0.15	-16.04	-0.15	-15.97	-0.15	-16.11
Age Group 60 or higher x LapseCycle	-0.29	-24.69	-0.29	-24.50	-0.29	-24.64	-0.29	-24.76	-0.29	-24.63
Lapse Cycle	0.11	8.81	0.10	8.24	0.13	9.85	0.10	8.25	0.10	6.21
Female	-0.02	-4.39	-0.02	-4.84	-0.02	-3.79	-0.02	-3.92	-0.02	-5.03
Female x LapseCycle	-0.01	-0.71	-0.01	-0.86	0.00	-0.63	-0.01	-0.81	-0.01	-0.84
Size less than 200k	-0.06	-6.58	-0.04	-4.37	-0.05	-5.72	-0.04	-3.97	-0.06	-6.30
Size 400k to 750k	-0.03	-4.13	-0.05	-7.34	-0.03	-4.84	-0.05	-7.60	-0.03	-4.83
Size 750k or higher	-0.01	-1.42	-0.06	-10.55	-0.02	-3.34	-0.07	-12.16	-0.02	-2.69
Size less than 200k x LapseCycle	-0.05	-3.29	-0.04	-2.89	-0.05	-3.20	-0.04	-2.93	-0.05	-3.10
Size 400k to 750k x LapseCycle	0.00	-0.38	-0.01	-0.84	-0.01	-0.46	-0.01	-0.89	-0.01	-0.57
Size 750k or higher x LapseCycle	0.03	2.71	0.02	1.62	0.03	2.49	0.01	1.20	0.02	2.18
Smoker	0.47	65.01	0.48	66.81	0.47	65.06	0.49	67.66	0.47	64.96
Smoker x LapseCycle	0.02	1.41	0.02	1.51	0.02	1.44	0.02	1.82	0.02	1.34
Risk Class (Better)	-0.22	-96.44	-0.23	-100.11	-0.22	-96.79	-0.23	-101.22	-0.22	-96.52
Risk Class (Better) x LapseCycle	-0.03	-9.12	-0.04	-9.61	-0.04	-9.30	-0.04	-9.88	-0.04	-9.31
ZIP Code Income <50k	0.19	28.72							0.15	18.38
ZIP Code Income 75k to 100k	-0.07	-12.39							-0.04	-6.08
ZIP Code Income 100k or higher	-0.20	-39.48							-0.10	-13.26
ZIP Code Income <50k x LapseCycle	0.04	3.91							0.03	2.06
ZIP Code Income 75k to 100k x LapseCycle	-0.02	-1.95							-0.01	-0.64
ZIP Code Income 100k or higher x LapseCycle	-0.04	-5.01							-0.01	-0.80
ZIP Code Minority < 10%			-0.10	-21.09					-0.08	-16.32
ZIP Code Minority >= 30%			0.22	42.34					0.13	23.02
ZIP Code Minority < 10%x LapseCycle			-0.03	-3.74					-0.02	-2.34
ZIP Code Minority >= 30%x LapseCycle			0.05	6.07					0.03	2.72
ZIP Code College+ < 25%					0.14	7.16			0.07	3.55
ZIP Code College+ 50% to 75%					-0.11	-18.76			0.02	2.29
ZIP Code College+ > 75%					-0.28	-46.76			-0.04	-3.82
ZIP Code College+ < 25%x LapseCycle					-0.02	-0.46			-0.03	-0.88
ZIP Code College+ 50% to 75% x LapseCycle					-0.03	-2.65			0.00	0.17
ZIP Code College+ > 75%x LapseCycle					-0.07	-6.53			-0.02	-1.30
ZIP Code HomeOwnership% < 40%							0.02	2.37	-0.04	-5.25
ZIP Code HomeOwnership% 40% to 60%							0.08	14.59	0.01	1.30
ZIP Code HomeOwnership% > 80%							-0.12	-23.11	-0.03	-5.99
ZIP Code HomeOwnership% < 40% x LapseCycle							0.05	3.79	0.03	2.73
ZIP Code HomeOwnership% 40% to 60% x LapseCycle							0.05	5.33	0.03	3.37
ZIP Code HomeOwnership% > 80% x LapseCycle							-0.02	-2.48	0.00	-0.11
Whole & Others	-0.15	-33.79	-0.16	-35.89	-0.15	-34.26	-0.16	-36.18	-0.15	-34.04
Whole & Others x LapseCycle	0.20	27.50	0.20	27.50	0.20	27.61	0.20	27.46	0.20	27.24
Shock Year	1.94	98.63	1.94	98.65	1.94	98.67	1.94	98.52	1.94	98.67
Shock Year x LapseCycle	-1.04	-28.09	-1.04	-28.03	-1.04	-28.11	-1.04	-27.96	-1.04	-28.08
Number of Subjects	845,026		845,026		845,026		845,026		845,026	
Number of Periods	6,301,978		6,301,978		6,301,978		6,301,978		6,301,978	